Naval Research Laboratory

Washington, DC 20375-5320

NRL/MR/6707--97-7910

Cyclotron Wave Electrostatic and Parametric Amplifiers

WALLACE M. MANHEIMER

Plasma Physics Division

GEORGE EWELL

Georgia Tech Research Institute
Atlanta, Georgia, 30332

February 28, 1997

REPORT DOCUMENTATION PAGE

Form Approved OMB No. 0704-0188

1. AGENCY USE ONLY (*Leave Blank*)	2. REPORT DATE	3. REPORT TYPE AND DATES COVERED
	February 28, 1997	Interim Report

4. TITLE AND SUBTITLE

Cyclotron Wave Electrostatic and Parametric Amplifiers

5. FUNDING NUMBERS

PE - 73

6. AUTHOR(S)

W.M. Manheimer and G. Ewell*

7. PERFORMING ORGANIZATION NAME(S) AND ADDRESS(ES)

Naval Research Laboratory
Washington, DC 20375-5320

8. PERFORMING ORGANIZATION REPORT NUMBER

NRL/MR/6707--97-7910

9. SPONSORING/MONITORING AGENCY NAME(S) AND ADDRESS(ES)

Office of Naval Research
Arlington, VA 22217-5660

10. SPONSORING/MONITORING AGENCY REPORT NUMBER

11. SUPPLEMENTARY NOTES

*Georgia Tech Research Institute, Atlanta, Georgia 30332

Material regarding the Russian contribution is available as "CWESA-High Sensitive Input Amplifier with Super High Self-Protection for Use in Radar and Communication Systems," Final Report by Vladimir Vanke and Istok Corporation, ONR contract N68171-95-C-9145. It is available from ONR or from Wallace Manheimer.

12a. DISTRIBUTION/AVAILABILITY STATEMENT

Approved for public release; distribution unlimited.

12b. DISTRIBUTION CODE

13. ABSTRACT (*Maximum 200 words*)

Cyclotron wave amplifiers were invented in both the United States and Russia in the late 1950's. While work in the United States was dropped in favor of solid state amplifiers, their development and use continues in Russia. This paper develops the basic theory of these amplifiers for western scientists and engineers, specifies the performance of several sample commercially produced items, and compares performance of these devices with theory. Applications of devices to real world radar systems and the resulting advantages are briefly discussed.

14. SUBJECT TERMS

Cyclotron amplifier
Low noise amplifier
Receiver protector
Parametric amplifier

15. NUMBER OF PAGES

69

16. PRICE CODE

17. SECURITY CLASSIFICATION OF REPORT	18. SECURITY CLASSIFICATION OF THIS PAGE	19. SECURITY CLASSIFICATION OF ABSTRACT	20. LIMITATION OF ABSTRACT
UNCLASSIFIED	UNCLASSIFIED	UNCLASSIFIED	UL

NSN 7540-01-280-5500

Standard Form 298 (Rev. 2-89)
Prescribed by ANSI Std 239-18
298-102

CONTENTS

CYCLOTRON WAVE ELECTROSTATIC AND PARAMETRIC AMPLIFIERS

I Introduction

Cyclotron Wave Parametric Amplifiers (CWPA's) and Cyclotron Wave Electrostatic Amplifiers (CWESA's) were invented in the United States and in Russia roughly simultaneously, in the late 50's and early 60's[1-18]. These are a unique category of microwave tube in which an electrostatic cyclotron wave is launched on an electron beam in an input structure, this wave is amplified in an intermediate structure, and then coupled out in an output structure. Typically the input and output structures are the same. While these tubes can in principle operate at any power level, they were primarily developed as reciever input amplifiers, that is the first amplifier that a signal in a radar or communication system encounters on reception. CWPA's and CWESA's have several advantages, including self protection from overloads, highly linear amplification, linear phase variation with frequency, and low noise figure (low noise temperature). The low noise temperature might at first appear surprising for a system using an electron beam generated by a thermionic cathode, but special techniques were successful in achieving 'beam refrigeration'.[16] Initial experiments in the United States were reasonably successful in achieving low noise amplifiers (noise temperature of about 100°K), with bandwidth of 5-10%. However nearly all early experiments were not at microwave frequencies, but rather at UHF.

Shortly after the initial development in the United State, all work on this topic was dropped in favor of solid state input amplifiers. However work on cyclotron wave amplifiers did continue in Russia, although this work was not widely distributed in the technical literature (either in the former Soviet Union or in the West). This work is the basis of many Russian components used in a variety systems, both military and civilian. Thus while westerners thought of microwave tubes as only the last stage of a transmitter in a microwave or rf system, with everything else solid state; many Russian system engineers thought of tubes for both the last stage of the transmitter and first stage of the receiver, with everything in between solid state. So far, roughly ten thousand of these tubes have been manufactured and are in various systems around the world, mostly in Russia and China. They are manufactured by the ISTOK Research and Production Company in Fryazino, about 30 miles northeast of Moscow. Today ISTOK sells about 250 per year as exports, and more are manufactured for use in Russia. The cost of each is roughly $10k. A few years ago, the Georgia Tech Research Institute (GTRI) purchased several for use in a pulsed Doppler X-Band radar. A photo of one of the devices, with a ruler with a centimeter scale is shown in Fig.(1.1); the tube weighs a few pounds and is easy to hold in one hand.

The cyclotron wave amplifier has a number of features which makes it very attractive. It is inherently a very low noise tube; the low noise temperature coming from actively cooling the beam. This is done in one of two ways. The original work in both the United States and Russia utilized the input coupler as the cooling mechanism[1,16,19,20]. Since the fast cyclotron wave on the beam is a positive energy wave, it can be cooled by active coupling to a dissipative structure. The other cooling mechanism is to propagate

Manuscript approved January 1, 1997

the beam into a region of decreasing magnetic field so as to adiabatically cool it. Thus noise temperatures, which one might initially suppose to be restricted to values larger than the cathode temperatures, are in fact between about 50°K and 300°K, which correspond to a noise figure varying from less than 1dB to perhaps 3.5dB. Other advantages of the device include linearity (because there is no longitudinal bunching of the beam), high gain, wide and electronically controlled dynamic range, self protection from microwave overloads, and extremely fast response where there is such an overload. Also the units are well matched to one another. In some cases, the receiver input device is not only a microwave tube, but is a combination of an initial tube amplifier, followed by a transistor amplifier. While the unit is typically large compared to transistor amplifiers used in western systems, it is generally comparable with the transistor amplifier plus receiver protector.

While totally solid-state receiver systems are common in Russia, the unique combination of advantages of the CWESA have resulted in its use in a number of Russian systems. For example, CWESA's are available for the fire control radar of the S300 PMU air defense and ATBM system shown in Fig. (1.2).[21,22] This radar is a pulsed Doppler radar designed to operate in high clutter and electromagnetic countermeasure (ECM) environments.

The initial cyclotron wave amplifier utilized a parametric amplification process in order to achieve the desired signal gain. This required an oscillating quadrupole rf electric field in the gain region, with all of the additional complexities of this separate rf system. The frequency of this pump signal is twice the electron cyclotron frequency, which is approximately twice the signal frequency. Such devices are called cyclotron wave parametric amplifiers (CWPA's). An alternative is the use of a quadrupole electric field which also has a sinusoidal longitudinal variation but no time dependence[16,23-28]. They are typically simpler in that the separate rf pump signal is no longer required. These are called cyclotron wave electrostatic amplifiers (CWESA's). The development of CWESA's has been carried out largely in Russia[25-28], although one early experiment was carried out in the United States[9]. The initial US experiment was carried out at 3.25 GHz but only achieved low values of amplification. Virtually all of these receiver devices produced and sold by ISTOK have been CWESA's.

This paper documents the theory and performance of cyclotron wave amplifiers, in order to make this knowledge generally available in the West. A companion work develops the theory of these devices at cyclotron harmonics. The theory of these devices is, in fact, fairly straight forward, since the electron beams are very tenuous, so their self fields are generally negligible. Thus, the waves on the beam concern simply the electron dynamics, and not the self consistency. Nevertheless, work in Russia[29-31] and the United States[32] has carried out some calculations including the self fields as corrections. While the self fields of the waves are negligible, the waves are set up, and interact with one another, through imposed electric fields. These interactions must be, and are properly accounted for.

Sections 2-5 discuss the theory of CWESA's and CWPA's. Section 2 discusses transverse electrostatic waves on the beam and derives the dispersion relation for the fast and slow cyclotron waves, and fast and slow synchronous waves. Section 3 discusses cooling of the beam. A diverging magnetic field cools both the fast and slow cyclotron waves (but not the synchronous waves). The coupler, on the other hand cools only the fast cyclotron wave, and it only at frequencies near the cyclotron frequency. Section 4 discusses the CWESA. Topics it discusses are the parametric amplification, noise factor, dynamic range, its role as a receiver protector, and the implementation of a tunable CWESA. Section 5 discusses the CWPA. Topics here are the parametric amplification, and the topics as regards the CWESA, but with two additions. The CWPA has the disadvantage compared with the CWESA that the idler radiation can interfere with the amplified signal. A solution to this problem is the 2 beam CWPA which is also discussed. Finally, the CWPA has the potential of developing into a very low noise millimeter wave amplifier, possibly even at frequencies as high as 94 GHz. This is also discussed in Section 5.

Section 6 and 7 concern experimental tests on CWESA's. Section 6 discusses tests at ISTOK, performed mainly as an experimental verification of the theoretical formulae developed here. These tests were done at S and C band. Section 7 discusses measurements made on an X-Band CWESA at GTRI. These tests were mainly to confirm its consistency with system requirements. Finally, in the Appendix, the power relations are derived for the transverse waves on the beam.

II Electrostatic Waves on the Beam

In this section we examine waves on a thin, low current pencil beam in a uniform magnetic field B in the z direction. The current is assumed so small that the self fields of the beam are negligible. While the beam does not produce any electric fields, it does, of course respond to electric fields externally imposed. To describe the modes on the beam, complex notation is used to describe the displacement perpendicular to the to z, the direction of propagation, that is $\zeta=x+jy$. For a circularly polarized displacement at frequency ω, the displacement is proportional to $\exp i\omega t$ for right hand circularly polarized waves, and to $\exp -j\omega t$ for left hand circularly polarized waves. The convention we use here is that ω is always positive.

If the velocity in the z direction is denoted v, the Eulerian displacement of the particle can be decomposed into a summation over right and left hand circular displacements,

$$\zeta = R_+(z)\exp j(\omega t-\beta_e z) + R_-(z)\exp -j(\omega t-\beta_e z) \qquad (2.1)$$

where $\beta_e = \omega/v$. Then if there is an electric field, the linearized equation for the particle displacement is given by

$$d^2R_\pm/dz^2 \; -j\,\beta_c dR_\pm/dz = -(e/mv^2)E_\pm \exp \pm j\,\beta_e z \qquad (2.2)$$

where $E_\pm = E_x + jE_y$. The E_+ has a time dependence $\exp j\omega t$, and correspondingly for E_-. For the case where there are no electric fields present, there are four solutions of the dispersion relation of the linear equation, Eq.(2.2). Assuming that the spatial dependence is proportional to $\exp j\beta z$, we find that $\beta = 0$ or $=\beta_c$. Thus the dispersion relation for the four solutions of Eq.(2.2) are two roots

$$\omega = \beta v \pm \omega_c \qquad (2.3a)$$

and the double (degenerate) root

$$\omega = \beta v \qquad (2.3b)$$

These solutions for ω however are only meaningful for these regions of $\omega\beta$ space where $\omega>0$. A plot of the resulting dispersion relation is shown in Fig.(2.1). The uppermost root is the fast (positive energy) cyclotron wave, the lowermost root is the slow (negative energy) cyclotron wave, and the middle two roots are the degenerate fast and slow synchrotron waves. If the motion is separated out into its eigenfunctions, we find that

$$R_\pm = R_{2\pm} + R_{1\pm}\exp j\beta_c z \qquad (2.4)$$

where $R_{2\pm}$ are the amplitudes of the synchronous modes of right and left hand circular polarization, and $R_{1\pm}$ are the amplitudes of the cyclotron modes of right and left hand circular polarization. The four independent modes allow the beam to be initialized in the four independent variables, the initial x and y positions, and the initial x and y velocities.

Note that there is no longitudinal spatial bunching associated with the motion of the electrons; the displacement is all in the transverse plane. Since longitudinal bunching is very often the dominant nonlinear process in electron beam devices, the absence of it means that microwave devices based on this transverse displacement will probably have characteristics which are extremely linear. This is in fact the case for CWESA's and CWPA's.

Also, since the waves are electrostatic, all group velocities are equal to the beam velocity v. Hence, as long as other electromagnetic waves at this frequency are eliminated (for instance by making the radius of the cylindrical conductor so small that they are cut off), no signals can propagate backwards. This eliminates internal feedback and absolute instabilities. Therefore, amplifiers based on these waves therefore should be, and are, very stable.

Finally, as is shown in the appendix, the period averaged power of each is given by

$$P_{1\pm} = \pm I_o U_o \beta_e \beta_c \left| R_{1\pm} \right|^2, \qquad P_{2\pm} = -\pm I_o U_o \beta_e \beta_c \left| R_{2\pm} \right|^2 \tag{2.5}$$

where I_o is the beam current and U_o is the beam voltage. In this case, the positive sign means that the power is added to the electron beam, and the negative sign means that the power is subtracted, that is the wave has positive or negative energy in the conventional sense.

III. Cooling of the Beam

One important characteristic of both the CWESA and CWPA is the low noise temperature. One might assume that the minimum noise temperature of the device would be the cathode temperature, since the beam is generated at this temperature, and one might expect this temperature to be added to any noise already on the signal to be amplified. However, this is not the case, since in these devices the beam is cooled in one of two ways. First, the beam may be cooled in the transverse direction by propagating it through a decreasing magnetic field (adiabatic cooling). Secondly, the beam may be cooled by passing it through a dissipative structure so that the noise on the beam damps out. We will discuss each of these active cooling technique separately.

A. Adiabatic Cooling of the Beam

When a beam with a transverse temperature, (typically the cathode temperature) propagates along a decreasing magnetic field, conservation of the adiabatic invariant requires that $v_\perp^2/B$ or $R_\perp^2 B$ = constant. Here $v_\perp$ is the perpendicular velocity of the electron, and $R_\perp$ is its Larmor radius. Thus as the beam propagates into a region of decreasing magnetic field, its transverse temperature obeys the relation

$$T_\perp/T_{\perp cath} = B/B_{cath} \qquad (3.1)$$

This adiabatic cooling scheme is used especially in the CWESA, where the cooling of the transverse temperature reduces the amplitude of both the fast and slow cyclotron wave. However the synchronous wave, which is characterized by a transverse displacement of the guiding center is not cooled . To reduce noise of cyclotron waves in CWESA, the cathode is placed in the region of the strong magnetic field created by an additional magnet. The magnetic field is then adiabatically reduced to the resonance value in the interaction region, as shown in Fig.(3.1). However it is important to realize that this cooling scheme works best for low frequency amplifiers, because the device operates at cyclotron resonance, so the magnetic field in the interaction region is specified. The amount of cooling then is determined by how much larger the field can be at the cathode; these fields are limited to a maximum of about 18 kG with modern rare earth magnets.

The additional strong magnet needed, and shown in Fig.(3.1) is just outside the vacuum jacket, but right next to the cathode and cathode heater. This puts a constraint on the heater power density and cathode temperature in such a confined configuration. As shown in the next section, a certain current (typically about 100-200 μA) is needed for optimum performance of the device (especially bandwidth). While a pencil beam could be used, the beam current density required is relatively high, implying a high cathode temperature and heater power. These requirements are not consistent with the geometric configuration shown in Fig.(3.1). One solution is to use a ribbon beam, giving a lower current density (i.e. lower cathode temperature) and correspondingly, a reduced heater power density, an approach now consistent with the geometric configuration shown. This technique has been pioneered at ISTOK and Moscow State, and is typically the most

difficult aspect of the engineering of the CWESA. Both the magnetic configuration and beam have to be very carefully designed, and designed in a configuration which has no symmetry, i.e. in an inherently three dimensional configuration[33,34]. When this is successfully done, there is no beam current collected at any point along the beam tunnel unless the device is operated as a receiver protector. The cyclotron waves on the ribbon beam, however, are essentially the same as those on the pencil beam.[35-37]

Finally note that these processes are much similar, but opposite to those which are usually used in gyrotrons. There the magnetic field increases along the orbit so as to increase the free energy for microwave generation. Here the magnetic field decreases along the orbit so as to reduce the receiver temperature and noise figure.

B. Noise Reduction in the Input Coupler

The input coupler is taken as being of the Cuccia type, basically a capacitor in a resonant cavity. In the capacitor, there are electric fields perpendicular to the plates; the rest of the cavity acts as a reactive and resistive element. A sketch of the coupler is shown in Fig.(3.2a), and a schematic of it in terms of an equivalent circuit is shown in Fig.(3.2b). Since the coupler is taken to be long compared to ω/v, it is the $k \cong 0$ mode which couples most strongly to it. As is apparent from Fig.(2.1), there is only one such mode (at least at non zero frequency), the fast (positive energy) cyclotron mode. Thus this coupler will be particularly effective in coupling to the fast cyclotron mode at the cyclotron frequency (ie at zero wave number). Furthermore, since the wave has positive energy, any dissipation in the circuit will tend to reduce the amplitude of this wave on the beam. By proper design of the coupler, it is possible to very greatly reduce the noise on the beam for frequencies near ω_c.

The equivalent circuit of such a resonant cavity coupler is shown in Fig.(3.2b). All the circuits (of the resonator and of the external load) are described here by the summary parallel conductivity Y_o. In order to describe the interaction of transverse waves of the electron beam with a resonant cavity coupler of this type, one may use the equations obtained earlier for the complex amplitudes of transverse waves

$$dR_{1+}/dz = (je/mv_z\omega_c)E_+ \exp j(\beta_e-\beta_c)z \qquad (3.2)$$

where only the fast cyclotron wave is considered. It is now necessary to determine the amplitudes of the circularly polarized components of the electric field $E_{\pm}$. Using the law of conservation for energy $dP_{circuit} = -dP_{beam}$, where P means power in the circuit or beam. Let U be the voltage across the capacitor, I the current in the circuit, and I_{in} the current induced in the circuit by the electron beam. Then:

$$UdI_{in} = -dqv_x(-U/d) = I_o dt v_x U/d \qquad (3.3)$$

so that

$$I_{in} = -(I_o/v_z d)\int_o^L dz\, v_x \tag{3.4}$$

and from the circuit model,

$$E = E_x = -I_{in}/dY_o\,, \quad I_{in} = I_{in+}\exp j\omega t + I_{in-}\exp -i\omega t \tag{3.5}$$

Then making use of

$$V_x = \frac{d}{dt}(\varsigma + \varsigma^*)/2 = (\frac{\partial}{\partial t} + V_z\frac{\partial}{\partial z})(\varsigma + \varsigma^*)/2, \tag{3.6}$$

and assuming only the fast cyclotron wave is present,

$$\frac{d}{dz}R_{\pm}(z) = j\beta_c R_{1\pm}(z)e^{j\beta_c z}, \tag{3.7}$$

we find that:

$$V_x = j\frac{\omega_c}{2}[(R_{1+}e^{-j(\beta_e-\beta_c)z} - R_{1-}^* e^{-j(\beta_e+\beta_c)z})e^{j\omega t} + (R_{1-}e^{j(\beta_e+\beta_c)z} - R_{1+}^* e^{j(\beta_e-\beta_c)z})e^{-j\omega t}]\,. \tag{3.8}$$

The expression for the induced current and electric field then involves the integral of v_x over the length of the coupler. Relating v_x to R (for the fast cyclotron wave), we have an expression for the electric field in the coupler in terms of the analogous integral of R. Then

$$dR_{1+}(z)/dz = -[I_o/4U_o d^2 Y_o]\{\exp j(\beta_e-\beta_c)z\}\int_o^L dz'\, R_{1+}(z')\exp -j(\beta_e-\beta_c)z' \tag{3.9}$$

Thus one obtains a physically clear result: this type of resonator can be efficiently used for selective interaction with the fast cyclotron wave of the electron beam. On integrating Eq. (3.9):

$$R_{1+}(L) = (1 - \frac{2G_e}{Y_\Sigma})R_{1+}(0), \tag{3.10}$$

where

$$Y_\Sigma = Y_o + Y_e\,; \quad Y_e = G_e + jB_e\,,$$

and

$$G_e = G_o[\sin\theta/\theta]^2 \qquad \theta = (\beta_e-\beta_c)L/2 \tag{3.11}$$

and

$$B_e = -2G_o \frac{2\vartheta - \sin 2\vartheta}{(2\vartheta)^2}, \quad G_o = (I_o/8U_o)(L/d)^2 \tag{3.12}$$

It follows from (3.10) that:

$$P_{1+}(L) = \left|1 - \frac{2G_e}{Y_\Sigma}\right|^2 P_{1+}(0), \tag{3.13}$$

where P_{1+} is the power in the fast cyclotron wave.

Thus Y_e defines the complex conductivity of the electron beam. At cyclotron resonance, the resistive part is maximum and the reactive part is zero. In order to minimize the noise on the beam at this frequency, it is straightforward to show that G_o = the real part of Y_o. Since the impedance is that of a resonant circuit, it also is purely real at the resonant frequency, assumed to be the cyclotron frequency. At frequencies near the resonance, the reactive part of the circuit conductance and beam conductance are linear in ω-ω_c. The fast cyclotron wave noise will be minimized over the largest possible bandwidth if these parts of the conductance are equal in magnitude and have opposite sign. Hence when

$$2G_e(\omega) = Y_\Sigma(\omega) \tag{3.14}$$

all the power of the fast cyclotron wave of the electron beam will be withdrawn from the beam and transmitted to the external circuit load. Thus, as far as the input resonator is concerned, noises of the electron gun on the fast cyclotron wave will be removed (withdrawn) from the beam, i.e. the electron beam on the fast cyclotron wave will be "cooled".

The condition, Eq. (3.14) corresponds to the requirement

$$Y_e(\omega) = Y_o^*(\omega) \tag{3.15}$$

In this way we obtain a well known physical result: all the power is transmitted from the generator (the fast cyclotron wave of the electron beam) in the external load when their conductivities are matched in a complex-conjugated way. In the presence of the external signal source the equivalent scheme shown in Fig. (3.3)should be considered. Applying a similar procedure we obtain:

$$P_{1+}(L) = \left|1 - \frac{2G_e}{Y_\Sigma}\right|^2 P_{1+}(0) + \frac{4G_L G_e}{|Y_\Sigma|^2} P_s, \tag{3.16}$$

where $Y_\Sigma = Y_e + Y_o$; $Y_o = Y_c + Y_L$. In this case:
$Y_c = G_c + jB_c = G_c + j(\omega_o C_c - 1/\omega_o L_c)$ is the equivalent conductivity of the circuit having the resonance frequency $\omega_o \approx (\sqrt{L_{\text{ñ}} C_{\text{ñ}}})^{-1}$ and the real reciprocal resistance G_c , $Y_L = G_L + jB_L$ is the equivalent conductivity of the signal source (signal generator or external load) in terms of the circuit conductivity. If the circuit is optimized, then

$$\omega_o = \omega_c,\ (G_{\text{ñ}} / G_o) \langle\langle 1,\ |B_L / G_o| \langle\langle 1, \qquad (3.17)$$

and the conditions of the optimal power transmission from the fast cyclotron wave to the load and vice versa are the same.

The requirements (3.16) and (3.17) determine the frequency band of CWESA couplers, which can reach 5-10%. This implies that the loaded Q of the cavity is in the range of 10-20, in comparison to the cold Q of the cavity which is typically several hundred. These relations have been tested many times over the years at ISTOK and Moscow State and have been found to be basically accurate for both pencil and ribbon beams. The effects of the self fields are almost invariably very small, as has been confirmed both by experiment and numerical simulations.

IV. The Cyclotron Wave Electrostatic Amplifier (CWESA)

This section considers the basic theory of the CWESA. It is divided into several subsections, the basic parametric instability, the noise factor of the device, the dynamic range, its role as a receiver protector, and a tunable amplifier variant.

A. The Parametric Amplification

The CWESA is a driven by a spatially varying electrostatic field at zero frequency. In the parlance of parametric processes, it is driven by a pump of zero frequency. This is a simplifying feature of CWESA's as compared to CWPA's. Since the pump field is at zero frequency, a parametric amplification can only proceed through the coupling of a positive and negative energy wave through the pump.

The spatially twisted electrostatic quadrupole field can be created by the quadrupole electrostatic spiral shown in Fig. (4.1). The quadrupole field is a solution of Laplace's equation, exhibiting a potential proportional to $I_2(kr)\cos(\beta_q z+2\theta)$. Expanding for $kr<<1$, we find

$$V(x,y,z) = V_{oe}\,[(y^2-x^2)\cos\beta_q z - 2xy\sin\beta_q z]\,/a^2 \qquad (4.1)$$

Taking the gradient of the potential to find the electric field, one obtains the electric field on the particle in terms of its displacement. The result is

$$E_+ = -2\,(V_{oe}/a^2)\zeta^* \exp j\,\beta_q z \quad \text{and} \quad E_- = -2\,(V_{oe}/a^2)\zeta \exp -j\,\beta_q z \qquad (4.2)$$

Since the electrostatic field a particle sees depends on its displacement, the quadrupole field couple various waves to one another if the frequency and wave matching conditions are met. In the case of a the coupling of the fast and slow cyclotron waves to one another, a fast cyclotron wave at frequency and wave number (ω,β) can couple through the stationary quadrupole field to a slow cyclotron wave at $(\omega, \beta+\beta_q)$. Thus as long as

$$\beta_q = 2\omega_c/v_z = 2\beta_c, \qquad (4.3)$$

the frequency and wave matching conditions are met for any ω. This then is the condition for the design of the quadrupole field in the CWESA. If this condition is met, the equations for the coupling of the fast and slow cyclotron waves turn out to be

$$dR_{1+}/dz = -j\varepsilon\beta_c R_{1-}^* \exp -j(\beta_q z - 2\beta_c z), \quad dR_{1-}^*/dz = j\varepsilon\beta_c R_{1+} \exp j(\beta_q z - 2\beta_c z) \qquad (4.4)$$

where $\varepsilon = 2eV_{oe}/ma^2\omega_c^2$. In Eq.(4.4), the exponential term is retained even though we have assumed that $\beta_q z = 2\beta_c z$. In this way, we not only show the effects of wave number mismatch, but we also point the way for a nonlinear calculation of the gain. In the

nonlinear regime, β_q is constant, but $\beta_c = \omega_c/v_z$ varies with z as the particle decelerates. The term $\beta_c z$ must be replaced with an integral over the velocity, where the nonlinear equation for the velocity of the particle must be solved in an additional calculation. From Eq. (4.4) we find that in the linear regime at resonance, there is an invariant:

$$\frac{d}{dz}\left\{|R_{1+}|^2 - |R_{1-}|^2\right\} = 0, \quad \text{or} \quad P_{1+}(z) + P_{1-}(z) = \text{const} \tag{4.5}$$

Thus the total energy of the electron beam is not changed in the process of interaction with the twisted quadrupole field of the electrostatic structure. The increase in energy of the fast cyclotron wave is always connected with the growth of the slow cyclotron wave, i.e. with the deceleration of the electron beam.

Solving the system of equations (4.4) gives:

$$\begin{aligned} R_{1+}(z) &= R_{01+}\mathrm{ch}\tau - jR^*_{01-}\mathrm{sh}\tau, \\ R_{1-}(z) &= R_{01-}\mathrm{ch}\tau - jR^*_{01+}\mathrm{sh}\tau. \end{aligned} \tag{4.6}$$

Here: $\tau = \varepsilon\beta_c z$; $R_{1+}(z=0) = R_{01+}$, $R_{1-}(z=0) = R_{01-}$ are the amplitudes of the fast and slow cyclotron waves, respectively at the input of the quadrupole section. Since at the output from the input resonator $R^{signal}_{01-} = 0$, the power gain of the fast cyclotron wave of the signal is equal to:

$$G_{(dB)} = 10\lg\frac{|R_{1+}(L)|^2}{|R_{1+}(0)|^2} = 20\lg\mathrm{ch}(\varepsilon\beta_c L), \tag{4.7}$$

where L is the length of the electrostatic gain region. Notice that there is no frequency dependence to the gain, and also any frequency can satisfy the frequency and wave number matching conditions for parametric instability. Thus the gain mechanism is inherently very wide band; the constraint on bandwidth of the amplifier comes from the bandwidth of the input and output structures.

Modern CWESA's often employ ribbon beams for a increased loading of the input and output resonators, i.e. to increase the value of the conductivity G_o introduced by the electron beam, by using intensive currents and small gaps between the resonator pads [see Eq. (3.12)]. In such amplifiers it is convenient to use plane periodic system Fig.(4.2) as an amplifying structure. The electric field potential in the vicinity of the axis of such a structure can approximately be described by an expression of the form:

$$V(x,y,z) = \frac{V_{oe}}{a^2}\cdot x^2 \cdot \mathrm{Cos}(\beta_q z), \quad \beta_q = 2\pi/L_g, \tag{4.8}$$

where V_{oe} is a certain effective potential dependent on the geometrical dimensions and on the potential V_o applied to the gain structure. If the electrostatic potential is

decomposed into its various circular polarizations, one can derive an equation for the coupling of the fast and slow cyclotron waves identical to Eq.(4.4) except that the coupling coefficient is now $\varepsilon = eV_{oe}/2ma^2\omega_c^2$, one fourth of the value for the case of only the circular polarization of the right helicity. Other components of the potential give rise to the possibility of coupling the positive energy cyclotron mode and negative energy synchronous mode, but are not encountered in practice. Since the wave matching conditions are quite different, these processes do not interfere with one another. Thus the field created by the plane periodic system contains several components, but under adiabatic ($\varepsilon<<1$) resonance interaction ($\beta_q = 2\beta_c, \quad \Rightarrow \quad \omega_e = 2\omega_c$) it is only one of these components that provides gain in much the same way (and by similar formulae) as in the case of the spatially twisted quadrupole spiral.

As for its design, a plane periodic structure can be relatively simple and consists of two binary combs inserted one into another with symmetrically opposite potentials Fig.(4.3). The scheme of connection of voltage supplies to such a system is similar to that shown in Fig. (4.2). The potential U_{os} determines the average velocity of the beam inside the gain region. In the low frequency part of the microwave arange (0.5-1.5 GHz), this potential is usually equal to that of the input resonators. For higher frequency devices, (6-12 GHz) it can be several times greater than the potential of the resonators so that the periodicity length of the plane gain structure L_g should have reasonable dimensions.

B. CWESA Noise Figure

Noise figure is normally defined as:

$$F(\omega) = [P_s/P_N]_{in} / [P_s/P_N]_{out} \qquad P_{N,in} = kT_o\Delta f, \quad T_o = 293^\circ K \tag{4.9}$$

where P_S, P_N are the signal power and the noise power in the narrow frequency band Δf, respectively. Using Eqs. (3.1), (3.16) and (4.6), we find:

$$F(\omega) = 1 + \{th^2\tau + |Y_\Sigma - 2G_e|^2/4G_eG_L\}\omega T_{cath}/\omega_{co}T_o \tag{4.10}$$

The first term in brackets makes allowance for the fact that in the process of electrostatic gain, in accordance with solutions Eq. (4.6), noise of the slow cyclotron wave of the electron beam enter the channel of the fast cyclotron wave. These processes are illustrated in Fig. (4.4)

The output resonator extracts from the electron beam the energy of the following fast cyclotron waves:

- Amplified fast cyclotron wave of the signal - $R^S_{01+}ch\tau$,
- Amplified fast cyclotron wave of the noises accompanying the signal - $R^N_{01+}ch\tau$,

- Amplified fast cyclotron wave of the noise $-jR^{*N}_{01-}\,sh\tau$, which arises in the process of electrostatic gain from the noise slow cyclotron wave R^{N}_{01-} existing in the beam at the input into the gain region. It should be stressed that R^{N}_{01-} does not interact with the input resonator and is not "cooled" in it. Thus the low noise temperature of the CWESA arises from the adiabatic expansion of the magnetic field, not from the Cuccia coupler.

The waves with the amplitudes $R^{N}_{01-}\,ch\tau$, $-jR^{*S}_{01+}\,sh\tau$, $-jR^{*N}_{01+}\,sh\tau$, that appear at the output of the gain region are slow cyclotron waves and do not interact with the output resonator. The minimum value of the noise coefficient is achieved by complex conjugate matching of conductivities as described in the last section. Hence we find

$$F_{min}(\omega) = 1 + th^2\tau \cdot \frac{\omega}{\omega_{co}} \cdot \frac{T_{cath}}{T_o}, \qquad (4.11)$$

here $th^2\tau \cong 1$, if the gain is greater than 10-15 dB.

Thus the problem of expanding the frequency bandwidth of CWESA is reduced to the problem of expanding the frequency band of the coupler. Our discussion of Cuccia coupler illustrates the main ideas that must be used in this case:

- The intrinsic frequency of the resonator is equal to the cyclotron frequency $\omega_o = \omega_c$,
- The slope of the curves $B_e(\omega)/G_o$ and $B_c(\omega)/G_o$ are chosen so that the total reactivity is equal to zero in the central part of the bandwidth. This requirement can be said to approximately correspond to that of cold loaded Q-factor of the resonator being numerically close to 1/6 of the transit angle:

$$Q_L \approx \frac{1}{G_o\sqrt{\frac{L}{C}}} = C\omega_o / G_o = \frac{1}{6}\frac{\omega_c L}{V_z} = \frac{1}{6}\theta_L, \qquad (4.12)$$

- The ratio of the active conductivities of the external circuit and that of electron beam

$$(G_{L+} + G_C)/G_o \approx 0.7 - 0.8 \qquad (4.13)$$

which allows additional (and noticeable) expansion of the frequency band as discussed in the section on the coupler.

C. Dynamic Range of the CWESA

In any input amplifier, an important consideration is its dynamic range, the range of input signal for which it operates as a linear amplifier. The lower bound is usually the noise level, and the upper bound is the start of nonlinear limitation of the signal. This

latter is generally defined as the maximum signal power for which the amplified power is within 1 db of its linear gain value, although there are a number of different definitions of dynamic range. There are two basic physical effects which limit the dynamic range. The first is beam interception of beam on the output resonator, and the second is nonlinear and beam thermal effects. Finally, we note that the dynamic range of the CWESA can in fact be varied electronically. We will discuss each of these.

1. Interception of the Beam in the Output Resonator

This will be the principal factor limiting the CWESA dynamic range where the amplification process is linear. The input aperture of the output cavity is usually equal to the distance between the resonator pads, and thus will limit the beam propagation above a certain threshold power, as shown in Fig.(4.5).

Taking into account the simplest geometrical considerations, one can derive an expression for the upper boundary of the dynamic range, i.e. for the maximum power of the fast cyclotron wave at the output to the cavity. The allowance should be made for the fact that at maximum power of the fast cyclotron wave, the slow cyclotron wave is present also. With gain coefficient of more than about 10 db, the amplitudes of these waves are about equal. Therefore the maximum deviation is given roughly by

$$|R_{1\Sigma}|_{max} = |R_{1+}| + |R_{1-}| \approx 2|R_{1+}|. \qquad (4.14)$$

and consequently the maximum signal power is about

$$P_{1+max} \approx \frac{1}{4} \cdot \frac{I_0}{2e'} \omega\omega_c (R_o - r_b)^2 . \qquad (4.15)$$

Taking the beam current $I_0 = 100\mu A$, the input aperture radius $R_o = 0.5mm$, the electron beam radius $r_b = 0.1mm$ and the working frequency $f = 5\ GHz$ ($\omega = \omega_c$), we find that: $P_{1+max} = 11.2\ mW$.

If the gain in signal power is equal to 20 dB, the maximum power of the input signal, that determines the upper boundary of the dynamic range, is equal to $P_{max} = 0.11mW$. This value is, of course, an estimation one, and can vary within a certain range owing to changes in corresponding parameters. However it is clear that one way of increasing the dynamic range of the CWESA is simply to increase the current. In doing so, the loading of the input cavity is unchanged as long as I/d^2 is constant.

2. Nonlinear and Thermal Effects

For the CWESA, electrostatic pump potential is given by Eq.(4.1). For a beam on the axis, there is no electric field in the z direction. However the device works by deflecting the beam off the axis and into regions where there is an E_z, that is into regions where they are accelerated or decelerated. This ultimately causes the resonance condition

for three wave interaction, Eq.(4.3) to be violated. It limits the gain and dynamic range even with no velocity spread on the beam, and limits it further if there is velocity spread.[38,39] An actual calculation of this effect would require a numerical calculation of the self consistent particle orbits. First, an approximate calculation for the scaling is given, and then results from numerical simulations done at Moscow State University are presented.

The electric field in the z direction is given by

$$dv_z/dt = 0.5\omega_c^2\varepsilon\beta_q[(y^2-x^2)\sin\beta_q z + 2xy\cos\beta_q z] \qquad (4.16)$$

The quantities x and y are obtained from $R_{\pm}$, the equations for these being given in Eq.(4.4). As v changes from its resonant value, Eq.(4.3), there is a phase mismatch. In terms of the phase mismatch, there is a small correction to the spatial growth rate given roughly by $(\beta_q-2\beta_e)^2/\beta_c\varepsilon$, the denominator being the spatial growth rate in the linear regime. Writing this phase mismatch in terms of δv_z, one can determine

$$\Delta\text{Gain} = \int dz\, 4\beta_c(\delta v_z^2)/\varepsilon v_o^2 \qquad (4.17)$$

where the integral is over the gain region and δv_z is the nonlinear change in parallel velocity. This comes from integrating Eq.(4.16). Inserting for x and y from the R's, one finds sines and cosines of various arguments. However certain of the trigonometric functions have arguments $(\beta_q-2\beta_c)$ (or more accurately, $\int dz(\beta_q-2\omega_c/v_z(z))$). These are slowly varying functions and give the main contribution to the expression for ΔGain. Approximating R as $R_o\cosh Kz$ (where $K=\beta_c\varepsilon$), and neglecting phase variations of the slowly varying trigonometric quantities, and assuming an amplification length Λ, we find that the reduction in gain scales as $\beta_c^4R^4\cosh^4K\Lambda/\varepsilon^2$. More accurate numerical simulations of the gain limitations at Moscow State university have, shown in Fig.(4.6) have calculated the ratio of nonlinear to linear gain to linear gain. The independent variable is the gain length, $\varepsilon\beta_c z$, the dependent variable is gain ratio, and these are shown as the parameter $q^2 = \beta_q^2\rho^2/\varepsilon$, where ρ is the initial displacement in the fast cyclotron wave counting both signal and noise. Figure (4.6), as well as the approximate analysis leading up to it, both show that increasing ε increases the dynamic range, and decreasing β_q does also. However since ω_c, the frequency to be amplified is fixed, decreasing β_q implies increasing v_z. Both these results are very reasonable; if one desires increased dynamic range, increase the interaction strength and increase the beam voltage.

The thermal spread on the beam also affects the dynamic range because different particles gain transverse energy differently depending on their initial perpendicular energy and gyro phase upon entrance to the interaction region. If the electrons are Maxwellian, and are emitted from the cathode at the cathode temperature, and have gyro phase distributed uniformly over 2π, then one can show that in the linear gain regime, the distribution of longitudinal energy at the end of the gain region is given by

$$W_n(y) = [\pi y y_{0n}]^{-1/2}\exp[-y/y_{on}] \qquad (4.18)$$

where $y = U_{os} - U$ and $y_{0n} = 4kT_{cath}(ct^2\tau - 1)/n$, $n = \omega_{co}/\omega$, and U is the longitudinal energy of the electron.

Simple estimations show that even at rather high levels of the input signal the velocity spread arises mainly due to intrinsic thermal vibrations in the beam. For example, for $T_{cath} = 10^3 K$, $ch^2\tau = 10^2$, $n = 5$, $P_{so} = 10^{-7} W$, $I_0 = 100\mu A$, we have $y_{on} = 6.9V$. As the working frequency of CWESA is increased, it is necessary to increase the average potential U_{os} of the gain region, so the gain structure should have reasonable dimensions. Particle simulations of the electron distribution function as a function of the length of the gain region have been carried out at Moscow State University. One typical result is shown in Fig.(4.7). For low gain, the distribution function follows the analytic result, but for higher gain, tails appear to develop on the distribution function. These enhanced tails can give rise to beam reflection and reduction of the dynamic range of the CWESA. These tails arise principally from the initial beam temperature, and are more pronounced at higher temperature. The schematic of the CWESA demonstrating particle reflection is shown in Fig. (4.8). Thus at low microwave frequencies (say 1-3 GHz), where n is very large, the beam remains cold after the amplification. Here it is easy to get low values of noise temperature, high gain and high dynamic range. However at the higher microwave frequencies (say 7-11 GHz), where n is necessarily smaller, and the beam temperature is therefore higher, it is generally more convenient to work at low values of total gain, 10-12 db, for instance. Additional gain at these frequencies is obtained by including a in the amplifier package. Such a device is called an Electrostatic Combined Amplifier (ESCA).

Note that while a number of different voltages have appeared in this analysis, all are low, less than a few hundred, and almost always less than 100 volts in practice. All the necessary voltages can be created by a compact solid-state voltage transformer placed under the CWESA cover. In this case there is only one voltage of the CWESA power supply, it can be a low voltage supply, and total d.c. power consumption, including the cathode heater, for CWESA does not usually exceed 1-2 W.

3. Electronic Control of the Dynamic Range:

Since the dynamic range of the CWESA depends on the various voltages, especially V_o and U_{os}, its operating dynamic range can be electronically controlled by varying these voltages. This can be done on a microsecond time scale, and usually this option is built into commercially manufactured versions. In order to amplify a larger input signal, typically the Voltage V_o is reduced so the gain is reduced (usually in units of 10db). In this way, larger input signals remain in the linear regime. However the lower input signal parts of the dynamic range i.e. the parts requireing most amplification then are usually lost, as the thermal noise at the output is not reduced from $kT_o\Delta f$. Therefore, when the amplification is reduced, noise figure typically increases. Thus this electronic

control does not usually extend the dynamic range, but it does move it around. In practice, this almost always turns out to be an important feature of the CWESA.

D. The CWESA as a Receiver Protector

When a powerful input signal (for example, that of an active or passive disturbance) is introduced on the CWESA input, the amplitude of the fast cyclotron wave and, hence, the electron displacement increase so rapidly that the electron beam is absent in the second resonator, see Fig. (4.9). In this case the electron beam will be totally intercepted by the input resonator pads and will change (increase) the value of VSWR (from 1.05-1.2 up to 20-30 and higher). Thus, the power input signal will be reflected from the CWESA input and will not damage the amplifier. Hence the electron beam, under this high input signal condition does not enter the input resonator; thus providing a reliable protection of the subsequent receiver stages against high power overloads in the input signal levels. Thus the CWESA can carry out the function not only of a low noise input amplifier, but also of a receiver protector. In many conventional radar and communication systems, this is performed by two separate pieces of equipment. Also, in conventional receiver protectors, the overload power is absorbed by the protector. Here is reflected, meaning that there is virtually never any chance of burn out even at very high power overloads. In some cases, at very high input power, there may be some signal leakage through unintended paths from the input to the output. In the microwave directed energy, HPM parlance, this is 'back door' coupling. In the cases where the a ESCA is used, and the high power pulse is known and predictable (for instance the radar transmitter pulse) this back door coupling of the radar transmitter to the receive can be eliminated by the use of a blanking pulse. That is, during the transmitted radar pulse, the transistor amplifier is simply turned off. In practice, this completely prevents any part of the transmitted pulse from interfering with the receiver, but does not close this 'back door' at other times.

The electron beam interception by the resonator pads is not dangerous also owing low values of the beam current and the accelerating voltage (usually less than 150μA and not higher than 50V). On removing the overload, the serviceability of CWESA is restored in a short period of time, roughly Q_L/ω, where Q_L is the loaded Q of the device. Since the loaded Q is small, typically 10 or 20, the restoration time after an overload is very short, typically 2-20 ns or less. This is probably the shortest restoration time of any available device today.

This fast response time has at least two possible advantages in modern radar systems. First of all, in a pulsed Doppler radar at high pulse repetition frequency, the recovery time of a conventional receiver protector can take up a significant fraction of the time between pulses, leading to increased eclipsing losses. Secondly, if it is required to detect or track a target at close range, a fast recovery time is necessary. For instance if the radar pulse is 1 μsec, the theoretical minimum range is about 150 meters. If the receiver

protector takes 2 μsec to fully recover, the closest one can see a target becomes 450 meters. However if a CWESA with a 20 nsec recovery time is used, the target can be seen at 150 meters.

E. The Cyclotron Wave Tunable Electrostatic Amplifier

As we have discussed, the main limitation on the bandwidth of the CWESA comes from the coupling structure and not the amplification process. The bandwidth of the parametric instability is quite broad. The Cuccia coupler is basically capacitive with resonant frequency at ω_c and at long wavelength $\beta \approx 0$. Instead of a Cuccia type of coupler one could use a traveling wave tube with a slow wave circuit included. Then, the fast cyclotron wave can interact with a waveguide mode[40]. Since this is a positive energy mode interacting with the slow wave circuit, the interaction does not lead to amplification. On a ω,β diagram, the coupling of the cyclotron mode with the Cuccia coupler is shown schematically in Fig.(4.10a), where the dot represents the dispersion relation of the coupler. The coupling with a slow wave mode is shown in Fig. (4.10b). Here the dotted line is the dispersion relation for the slow wave mode. This slow wave is set up with a comb structure along one of the walls of the waveguide, as shown in Fig . (4.11a), with a schematic of the tunable CWESA shown in Fig. (11b). Typically, in practice, the speed of the slow waves is about one half or one third the speed of light. In tuning the CWESA, the voltage of the electron beam is varied in the coupling region, as is also illustrated in Fig. (4.10b). However the voltage in parametric amplification region is fixed by the condition $2\omega_c/v_z = \beta_q$. Thus the tunable CWESA has accelerates or decelerates the beam before it enters the coupling structure, and then accelerates it to the resonant velocity at the input to the quadrupole region. At the output coupler, it does the reverse. Such a tunable CWESA has been set up at Moscow State university and ISTOK. It has demonstrated very rapid electronic tuning capability over a range of about 50%, whereas the instantaneous bandwidth is about 1%.

V. The Cyclotron Wave Parametric Amplifier (CWPA)

While the CWESA used a time independent spatially periodic electrostatic field to couple the fast and slow cyclotron wave to give amplification, the CWPA uses a time varying quadrupole electric field to provide amplification. The field oscillates in time at twice the cyclotron frequency, so that it couples two positive energy waves at about the cyclotron frequency. While this amplifier is less frequently used than the CWESA, it was in fact the first one to be developed, both in the United States and in Russia. In this section we will discuss the basic amplification mechanism; the noise temperature, dynamic range, receiver protection, and tunable versions; a two beam CWPA which can eliminate the idler signal (that is the signal at the pump frequency minus the signal frequency); and the prospects of CWPA's at millimeter wavelength.

A. The Parametric Amplification Process

The electron rotating with a cyclotron frequency and entering the quadrupole field at the optimal phase (Fig.5.1) will be subjected to the action of the tangential accelerating force and its rotation radius will be increased. The potential of such a high-frequency quadrupole field has the form:

$$V(x,y,t) = \frac{V_o}{a^2}(x^2 - y^2)\cos\omega_p t, \qquad (5.1)$$

where ω_p is the pump frequency.

If the pump frequency is twice the cyclotron frequency,

$$\omega_p = 2\omega_c . \qquad (5.2)$$

then two fast cyclotron waves satisfy the frequency and wave number matching condition for parametric amplification. Because the pump is now at non zero frequency, there is an additional wave, the idler at frequency

$$\omega_i = \omega_p - \omega . \qquad (5.3)$$

which is also amplified. The wave number matching condition is that $\beta_i = -\beta$, since the quadrupole coupler now has zero wave number. A calculation completely analogous to that in Sec 4A shows that the growth rate for the CWPA parametric is still $\varepsilon\beta_c$.

In actual parametric amplifiers the high-frequency quadrupole field is usually created with the help of the microwave resonator with four pads (Fig. 5.2). As with the case of the CWESA, the parametric amplification itself is very wide band, and in fact as in Sec IVA, the growth rate has no dependence on frequency. However since the frequencies must now add up to ω_p (which is equal to $2\omega_c$), and since the fast cyclotron waves all have positive frequency, the frequency and wave number matching conditions can only be satisfied for frequencies between 0 and $2\omega_c$. This is somewhat more

restrictive than for the CWESA, although in practice, the device works only in a much narrower frequency band determined by the coupler.

The calculation of the fields in the cavity is not especially simple as it is electrostatic in the inner region, in the configuration in Fig. (5.2), since the dimension is much less than a free space wavelength, but like a resonant cavity mode in the outer region. However if a configuration like Fig. (5.1) could be set up, where the field is entirely electrostatic, calculation of it is quite simple. At microwave frequencies, solid state sources are available which easily have sufficient power to excite the parametric instability with reasonable spatial growth rate. To see this, consider the spatial growth rate, $2eV_o/ma^2\Omega_c v_z$. If we assume $\omega=6x10^{10}\,s^{-1}$, V_o of 10 Volts, a of 1 mm, and a 100 volt beam, we find a spatial growth length of about 1 mm. If the length of the interaction region is about a centimeter, the total electrostatic energy is about $4x10^{-12}$ Joules. If the configuration is as in Fig. (5.1), this is the total energy. However if the configuration is as in Fig. (5.2), there is also the electromagnetic energy in the outer region to consider. The fields are much lower here, for two reason, first the fields are enhanced by the sharp corners, and second, if the cavity is considered analogous to a transmission line, the voltage drop is across a smaller spatial distance. However the volume of the outer cavity is also greater. If we assume the total field energy is ten times the energy in the electrostatic inner region, and the cavity Q is 1000, as is reasonable for an X-band cavity, the power to generate the pump field in the cavity is only a few milliwatts.

One characteristic of the CWPA not found in the CWESA is the presence of the idler wave at nearby frequency and wave number. In the CWESA, there is an idler slow cyclotron wave, at exactly the amplified frequency, but at a wave number so different that it does not interact with the output coupler, and therefore does not interfere with operation of the device. Typically, in a microwave receiver, after the amplifier there is a mixer and heterodyne system where the amplified wave is converted to a lower frequency wave; this low frequency wave is separated from everything else by passing it through a low pass filter. If the idler wave of the CWPA is close enough to the signal frequency that it passes through the low pass filter as well, it interferes with the operation of the receiver. Therefore, unless corrective measures are taken (see Sec IVC), there is a small region at the center of the band where the CWPA is not usable. Generally this is a disadvantage to CWPA's as opposed to CWESA's.

B. Other Aspects of CWPA's

1. The Input and Output Coupler

The input and output couplers of the CWPA are also Cuccia couplers and as such, they cool fast cyclotron wave at wave numbers near zero. Since only fast cyclotron waves are involved in the CWPA, both the signal and idler waves are cooled by the input coupler. This is in contrast to the CWESA, where the idler is not cooled by the coupler. To cool the noise in the idler channel, the CWESA relied on adiabatic expansion of the beam between the cathode and input coupler. This required a large supplementary

magnet outside the vacuum jacket, right near the cathode. This was the feature of the CWESA which drove Moscow State University and ISTOK to develop ribbon beams. For the CWPA, there is no need for this extra magnet, since adiabatic cooling is no longer required. Correspondingly, CWPA's usually do not use ribbon beams, but typically use pencil beams of higher current density (but comparable current).

Early experiments on CWPA's in both the Untied States and Russia showed that it is very easy to cool the beam. Amplifier temperatures of about 50° K were easily achieved in early experiments in both nations. Bandwidths of CWPA's, restricted only by the coupler, are as in CWESA's.

It is also possible to use the tunable coupler (See Sec IVE) with parametric amplifiers. Thus one could make a tunable version, with a rapid electronic tuning range of about 50%, and an instantaneous bandwidth in the range of 1%.

2. Noise Figure and Dynamic Range and Receiver Protection:

Early experiments on CWPA's in both the united States and Russia showed noise temperatures lower than 50°K, (a noise figure of 1.2db) could easily be achieved. It is easier to reduce the noise temperature of CWPA's than of CWESA's because the idler wave is cooled in the former by the input structure. In the CWESA, noise from the slow cyclotron wave appears in the fast cyclotron wave channel after amplification. This slow wave is only cooled by adiabatic cooling. However adiabatic cooling becomes less effective at higher frequency, because the magnetic field in the amplification region ultimately will approach the field in the cathode region. Thus for high frequency low noise amplifiers, ultimately it will become more advantageous to use CWPA's rather than CWESA's.

As discussed earlier, the dynamic range of CWESA's is limited by two separate effects, beam interception by the output coupler pads, and nonlinear electron dynamics in the amplification region. Contributing to the latter are both the deceleration of the beam due to the axial electric field and also the effect of velocity spread on this nonlinear deceleration. The effect of beam interception should be about the same for both devices since the coupler is the same for each. However the beam nonlinear dynamics depend on the axial component pump electric field. It is only the CWESA which has an axial component of the pump electric field, the CWPA does not. Thus if the device is run in a regime where nonlinear effects, rather than beam interception determine the dynamic range, the CWPA should have a larger dynamic range than the CWESA.

However there is another consideration as regards the dynamic range of the CWPA. Here the power to the amplifier is ultimately the power going into the pump radiation at $2\Omega_c$. If the power of the amplified signal approaches this, there will be reduction of gain, or pump depletion in the terminology of parametric instabilities. This is simple conceptually to calculate. The pump power must supply not only $\omega W/Q$ (W is the stored energy in the cavity), but also the power going into the amplified signal, or

$$P = \omega W/Q + 2P_{1+} \qquad (5.4)$$

where the factor of 2 comes from the presence of the signal and idler. As a simple illustrative example, let's say that P_{1+} is 5% of the input power. Then the electric field of the pump is reduced by about 5%, or the growth rate is reduced by 5%. In 2 e-folding lengths, the power output is reduced by about $e^{0.2}$ from the linear value. This is about the 1 dB compression point. Thus as a rule of thumb, the CWPA will be linear as long as the amplified power is less than about 5% of the pump power, or the input power is down by a factor of about 10^{-3}.

As far as receiver protection is concerned, since the input coupler works the same way for both CWESA's and CWPA's, their properties as regard receiver protection should be about the same.

C. The Two Beam CWPA

We have seen that one of the principal difficulties of the CWPA as compared with the CWESA is the presence of the idler channel which can interfere with operation of the device. It is possible to eliminate this idler channel with the 2 beam CWPA, developed at Moscow State University and ISTOK[41]. In such a device, there are two separate electron beams, which are coupled to the input and output as in the one beam device. However each beam interacts with a different pump field, these two pump fields having the same amplitude, but 180° out of phase. Then the phase relations for parametric amplification show that if the signal is injected onto both beams with the same phase, the two separate idlers, as they grow exponentially on the two beams will be 180° out of phase. Thus when the signals on the two beams are recombined in the output cavity, the signal amplitudes add, but the idler amplitudes cancel. A basic schematic of the two beam CWPA is shown in Fig. (5.3)

D. The Prospect of Millimeter Wave CWPA's

We discuss here the possibility of low noise cyclotron amplifier at millimeter wavelengths. We consider principally the possibility of a CWPA input amplifier at 94 GHz, because there is now a national program in the United States to develop high power 94 GHz radars. Many components of such a radar, including receiver protectors at high transmitter power and low noise amplifiers are not at present optimally developed. It si especially interesting to consider a 94 GHz CWPA as a component to this radar. (Naturally, at other important, but lower millimeter wave frequencies such as 35, 44 and 60 GHz, development of a CWPA or CWESA would be easier.) A 94 GHz radar will require extremely high pulse repetition frequency (PRF) in order to provide adequate Doppler space for clutter suppression, and therefore must use a receiver protector with very fast recovery time (t<100ns). Also it must be capable of working at high transmitter

power. Furthermore development of a low noise input amplifier is especially attractive, because existing input transistor amplifiers and input mixers at these frequency typically have large noise figures, of order 5db or more, at least if they are not cryogenically cooled. Since the CWPA has the perhaps unique possibility of satisfying all of these requirements, it could be of very great interest of the U.S. high power 94 GHz radar program. Additionally, a low noise amplifier at 35 or 44 GHz could be of interest for space based communication systems. It may be that cyclotron wave amplifiers, assuming they could be developed, could providevery attractive options for a number of millimeter wave systems.

The cyclotron wave parametric amplifier does require a pump source at twice the cyclotron frequency, that is a frequency from 70-190 GHz depending on the operation frequency. In the lower range, GaAs Gunn oscillators generate out powers greater than roughly 100 mW at 35 GHz and 30 mW at 100 GHz. Gunn oscillators based on InP can provide much higher power at higher frequency, almost certainly in excess of 10 mW at 200 GHz. Both of these are easy to phase lock, an important consideration for a low noise amplifier. For instance the Hughes Series 4774xH phase locked Gunn oscillator has phase noise 60 db down from the carrier at a frequency 10 Hz away from the main signal 100 GHz, according to the Hughes catalog. The amplitude noise is smaller still.

Impatt diodes have much greater power, in excess of 100 mW at 200 GHz. However, at least when operated as free running oscillators, they have greater phase noise than Gunn oscillators. It may be possible to phase lock these as well. To summarize, pump sources with frequencies up to 200 GHz seem to be available to power millimeter wave CWPA's.

A cyclotron wave amplifier at 94 GHz would require a magnetic field of about 35 kG. We only consider here CWPA's, because the alternative, CWESA's would most likely require too large a magnetic field at the cathode to be of interest for a low noise amplifier. There are two possible approaches to the development of millimeter wave cyclotron amplifiers, the use of such large magnetic fields, and the possibility of cyclotron harmonic operation, which could lower the required field. We discuss here only the former, the latter will be considered in another publication. There are two approaches to the generation of such large fields, superconducting magnets and permanent magnets which concentrate the flux.

1. Superconducting Magnets

Superconducting magnets can generate the 35 kG fields quite easily. However to do so typically has required large systems with liquid helium. Advances in high temperature superconducting technology and advances in cryo-coolers have simplified the design of these magnets considerably[42]. At least at this time, it appears that conventional low temperature superconducting material is optimum for manufacturing the main magnet coil if the field desired is 35 kG. However with the use of high temperature superconducting magnetic material for the leads, it is possible to operate with only a cryo

cooler in a liquid helium free environment. The Intermagnetics corporation of Latham, New York has developed such a system. One particular such superconducting magnet has a bore 5 cm in radius and 10 cm long, and achieves a maximum field of 50 kG. The superconducting magnet is about 2 feet high, is about 8 inches in diameter, and weighs about 50 pounds. However since the volume of magnetic field is quite large compared to what is needed for a 94 GHz CWPA, it is likely that the size of the system could be very considerably reduced. Since the magnet bore would almost certainly have to have radius at most half a centimeter, and length at most 2 cm, the magnet size and weight could most likely be considerably reduced. It seems reasonable to think that a superconducting magnet for a 94 GHz CWESA could be developed with a weight of less than 20 pounds. While this is heavy compared to CWESA's that exist at lower frequency, it is no so much so as to be an overwhelming obstacle to its use. If one is willing to use modern superconducting magnets, low noise CWPA's which have reasonable size and weight could be developed.

Another approach to a superconducting CWPA is the use of cold, thermally isolated field coils. Here one cools the coils down to a superconducting temperature for either a high or low temperature superconducting material. Then one thermally isolates the coils as well as possible and runs the magnet until the coils warm up to a temperature near appropriate the transition temperature. At this point one takes out the coils and replaces them. Initial estimates at IGC corporation show that these coils could hold their charge for several months, and perhaps as long as a year before they would have to be replaced. However the reliable manufacture of such thermally isolated coils would still take some development.

2. Concentrated Field Permanent Magnets

With rare earth permanent magnets, it is now possible to arrange permanent magnets in a configuration which concentrate the fields. The rare earth permanent magnets are characterized by a remenance field B_r. This is essentially the field that it generates after it is magnetized, but in the absence of applied field. As of about the fall of 1996, the maximum remenance field is roughly 13 kG, and this value seems to be increasing slowly in time.

One such rare earth magnet configuration which concentrates the field is a Halbach cylinder, or magic cylinder[43,44]. This is a cylindrical configuration of rods of permanent magnets, magnetized perpendicular to its axis as shown in Fig.(5.4). If the permanent magnet fields are properly oriented, a uniform magnetic field B_w is produced inside the cylinder, perpendicular to its axis. If the cylinder has inner radius R_1 and outer radius R_2, the uniform field in inside the is

$$B_w = B_r \ln(R_2/R_1) \qquad (5.5)$$

and it is oriented perpendicular to the axis. Notice that not only can the field be larger than the remenance field, it can actually increase without limit as R_2/R_1 does. However

such an increase in central field does imply heavier and heavier structures. Nevertheless these structures can be built, and they, and structures approximately like them are being marketed commercially[45].

An analogous structure a three dimensional version called the magic sphere[46,47], shown schematically in Fig. (5.5). This also produces a uniform magnetic field in a spherical gap inside a larger sphere of magnetic material put together with their fields properly aligned. Its application in a microwave tube such as a CWPA is shown schematically in Fig. (5.6) While these have not yet been manufactured, either commercially or in the laboratory, their properties have been calculated for many possible configurations, and it should be possible to manufacture and market them. One of the most difficult obstacles to their manufacture is getting these magnets, which repel or attract each other, to stick together in the proper configuration. However, there are several approaches to doing this, and it does not appear to be an insurmountable obstacle. If the entire inner spherical gap is not needed, and it would not be needed for a CWPA, the magnetic field could be enhanced in a number of ways. Shown in Fig.(5.7) is the gap field in, as a function of radius ratio for a rare earth magnet with B_r=12 kG, with various enhancements to the inner field. With a permendur insert, a 35 kg field would be generated in a 1 cm radius gap, with a 6 cm outer radius sphere. The mass of the magic sphere has been calculated to be about 3-5 kg. Such a magic sphere permanent magnet structure could be the basis for the development of low noise CWPA's at 94 GHz.

VI Experimental Tests of the CWESA at ISTOK

This section presents experimental results for gain, noise and dynamic characteristics of two CWESA samples (variants 1 and 2) designed for operation at S and C band. It also briefly gives the characteristics of a new development at ISTOK, receiver protectors (without amplification) at K_u and K_a band.

A. CWESA Descriptions

The CWESA magnetic system utilizes permanent Sm-Co magnets and an additional magnet in the cathode region which provides the required profile of the longitudinal magnetic field along the amplifier axis, i.e. a high value of B_{cath} on the cathode surface, the adiabatic decrease in the drift region and the resonant value of B in the regions of both the couplers and the gain structure. The value of B_{cath} reaches 1.85±0.09 Tesla, and the magnetic field ratio is up to 10-20 in S and C band ranges. The magnetic field is stabilized against changes in thermal and temporal operation regimes of the amplifier and provides the necessary conditions to optimize the set of output characteristics of CWESA. Engineering the permanent magnet system is often the most challenging part CWESA design at ISTOK.

The plane cathode electron gun forms a thin ribbon-like electron beam (the cross-section at the cathode being 0.03 mm x 0.7 mm). The high value of microperveance of the electron gun (up to 3-5 $\mu A/V^{3/2}$) provides the beam current value of 250-280 μA at the values of potential about 15-18 V. The Cuccia coupler with the uniform transverse electric field is employed for the input and output CWESA resonant couplers, Fig.(6.1) . Here L and s are the length and width of the coupler pads, d is the gap between the pads where the transverse electric field is excited. The electron transit angle per the length is about 60-80 radian. The values of s and d are chosen taking into account the increase of the electron beam cross-section in the drift region with the divergent magnetic field. The value of d is about 0.2-0.3 mm, which provides the effective coupler loading by the electron beam.

In the two studied CWESA samples a plane periodic structure consisting of two binary combs inserted one into another is used as an amplifying system. Figure (4.2) illustrates the main parameters of the gain structure, here L_g and L_2 are the period and total length of the gain structure, s_2 is the tooth width, d_2 is the gap between the teeth forming the transit channel for the ribbon electron beam. The potential $\pm V_o$ required for exciting the quadrupole component of the electric field in the transit channel, is applied to alternating pairs of teeth belonging to the opposite combs of the structure. The whole structure is at the synchronism potential U_{os}. The potential U_{os} is usually equal to that of the input and output couplers in the low-frequency range, (0.5-1.5 GHz). For higher-frequency variants of CWESA this potential may be several times greater than that of couplers, so that the gain structure period should have reasonable dimensions. The CWESA collector has the potential greater than that of the couplers, which makes

it possible to prevent the reverse current of secondary emitted electrons from collector surface.

Table 6.1 lists the main parameters of two CWESA's under study.

Table 6.1

CWESA parameters	Variant 1	Variant 2
λ- wavelength band , cm.	10.5	4.4
I_o- electron beam current, μA	280	250
δ- electron beam thickness at cathode, mm	0.030	0.030
s_1 - electron beam width at cathode, mm	0.7	0.7
U_o - coupler voltage, V	18	15
L - length of coupler pads, mm	8	4.5
d- interaction gap of couplers, mm	0.27	0.18
s - width of coupler pads, mm	3	2
U_{os} - gain synchronism voltage, V	95	86
V_o- gain voltage, V	41	21
L_2 - gain structure length, mm	11.5	7
L_g - gain structure period, mm	1	0.4
d_2- interaction gap of gain structure, mm	0.5	0.18
s_2 - width of gain structure tooth, mm	0.4	0.14
n- magnetic field ratio	18.4	7.8
T_{cath}- cathode temperature, ^oK	1000	1000
Q_o unloaded Q	500	500
Q_L loaded Q	12	18
Approximate weight kg	2	2
Approximate volume liters	1	1

B. CWESA Gain as a Function of Gain Voltage and Operational Frequency

In section 4 the theoretical expression was derived for gain of a fast cyclotron wave power in CWESA:

$$G(db) = 20 \log ch(\varepsilon\beta_c L_2) \qquad (6.1)$$

from which it follows that is independent of the signal frequency and grows with increasing gain potential applied to the gain structure. In section 4C we considered main reasons responsible for limiting the CWESA, namely, electron beam interception, dynamic beam deceleration, etc. Below main theoretical conclusions are compared with the results of gain measurements for two CWESA variants.

For the chosen CWESA parameters (see table 6.1) the calculated values of ε are at the level of 0.05 (variant 1) and 0.033 (variant 2). The corresponding values of the dynamic beam deceleration parameter (see Sec 4.C.2) are $q = 4x10^{-3}$ and $1.6x10^{-2}$. The experimental dependencies of CWESA gain on the potential for variants 1 and 2 are shown in Fig. (6.2). The growth of gain with increasing V_o takes place in a good agreement with the expression Eq.6.1) up to the values of V_o =50V (variant 1) and V_o =23 V (variant 2). The maximum gain of the samples, however, did not exceed 15.5 dB (variant 1) and 11.5 dB (variant 2), although the influence of the dynamic deceleration of the electron beam (see section 4) is insignificant and allows the gain level of 20-25 dB to be realized. The observed limitation and subsequent drop in gain with a further increase in the potential V_o are caused by beam interception at the pads in the output coupler, since the size of the gap between the pads was left equal to that of input coupler in order to enhance the load by the electron beam and to realize the optimal noise characteristics of CWESA over a wider frequency range.

At the same time, the gain of 10-12 dB is quite acceptable for all the principal characteristics of CWESA to be maintained, while it is reasonable to obtain additional 10-15 dB with the help of a supplementary gain stage - a transistor amplifier included in the package (i.e. making it a ESCA). Once again, is the result of the particular engineering policy aimed at optimization of the unique set of gain, noise, dynamic and protecting characteristics of CWESA.

The synchronism potential U_{os} determines the average velocity of the electron beam within the gain region and, consequently, ensures fulfilment of gain resonance conditions

$$\beta_q = 2\beta_c \qquad (6.2)$$

The experimental dependencies of CWESA gain as a function of the potential for variants 1 and 2 are represented in Fig.6.3. The values of the potential, as calculated from the exact synchronism conditions (6.2), are 92.3 V and 83.0 V (variants 1 and 2, respectively) and are in a good agreement with the optimal values of (95 V and 86 V) obtained by experiment.

As discussed earlier, the power gain of the fast cyclotron wave is independent of frequency. However, the resulting CWESA gain can be represented as the product of the factor of signal transmission into the electron beam in the input coupler, of the factor of signal extraction out of the beam in the output coupler and of the signal power gain in the gain structure :

$$G(\omega) = K_{in}(\omega)\, G\, K_{out}(\omega) \qquad (6.3)$$

where K_{in} and $K_{out} = 4G_L G_e / |Y_\Sigma|^2$ are determined by matching the conductivities in the input and output couplers. The value of conductivity G_o inserted into the coupler by the electron beam plays a decisive role in extending the operational bandwidth of CWESA.

For the tested CWESA samples the values of G_o are 1.7×10^{-3} Ohm^{-1} (variant 1) and 1.3×10^{-3} Ohm^{-1} (variant 2). The measured values of unloaded quality factors Q_o of the couplers for both CWESA variants are nearly the same (of the order of 500), but the values of cold loaded quality factors Q_L of the couplers are 12 and 18 for variants 1 and 2, respectively. Estimations of loss conductivities in the couplers give the values about 2.9×10^{-5} Ohm^{-1} for variant 1 and about 3.7×10^{-5} Ohm^{-1} for variant 2, in this case the values of $G_L + G_C$ are about $0.71G_o$ and $0.79G_o$ respectively. The transit angles of the couplers are 56.9 radian (variant 1) and 83.1 radian (variant 2) which are close to the optimal values required, $\theta_l = 6[(G_L+G_C)/G_o]Q_L$ for complete compensation of the reactive component $B(\omega)$. Thus the conditions necessary for extending the bandwidth of the couplers are fulfilled (see 3.4.22 - 3.4.23). Figure (6.4) represents the measured frequency dependencies of VSWR of input couplers for both CWESA variants. Output couplers have similar frequency characteristics of VSWR.

The measured signal losses characterizing the value of the product $K_{in}(\omega)\, K_{out}(\omega)$ at the central frequency of the operating band for the tested CWESA samples were about 0.8 dB and 0.5 dB, which is consistent with theoretical estimations of 0.4-0.5 dB. The measured dependencies of CWESA gain on the signal frequency are shown in Fig. (6.5). The gain bandwidth is up to 12% and 6% for variants 1 and 2, respectively, and as one can see from comparison with the VSWR curves in Fig. (6.4), is determined by the bandwidth of the couplers. The narrower frequency band for variant 2 is due to a slightly larger transit angle of the couplers (as compared with variant 1) and relatively low loading by the electron beam.

C. CWESA Noise Factor as a Function of Operational Frequency

As shown in Section 4, noises at the CWESA output consist of two main components: noise of the fast cyclotron wave accompanying the signal, and noise of the slow cyclotron waves inserted into the fast cyclotron wave channel during the electrostatic amplification process due to the active coupling between the fast and slow cyclotron waves. The fast cyclotron wave noise at a particular point of the frequency range can almost completely be removed out of the beam at the input coupler by complex-conjugate matching of the conductivity, contributed by the electron beam with the summary circuit conductivity. In this case the minimal value of the CWESA noise factor is determined by the reduced level of slow cyclotron wave noise, R_{o1}^{N} which are not removed out of the beam in the input coupler:

$$F_{min}(\omega) = 1 + (th^2\tau)\omega T_{cath}/\omega_{co} T_o \qquad (6.4)$$

where $\tau=\varepsilon\beta_c L_c$ is the gain parameter (and usually $th^2\tau=1$), ω_{co} is the value of the cyclotron frequency at the cathode surface, T_{cath} is the cathode temperature, $T_o = 293$ K. Besides the noise factor, the input amplifier is often characterized by the noise temperature T_{noise}. For CWESA the minimal noise temperature is equal to:

$$T_{noise,min} = (th^2\tau)\omega T_{cath}/\omega_{co} \qquad (6.5)$$

Application of Sm-Co magnets, optimization of the cathode unit design and optimization of the shape of additional magnet forming the field near the cathode, make it possible to achieve the values of of the order of 1.8- 1.9 Tesla. This provides high values of the magnetic field ratio (up to 18 for variant 1) and creates conditions for achieving the values of F_{min} of about 1.15-1.20.

The value of the magnetic field ratio in the CWESA decreases with frequency due to the limitation of accessible values of the magnetic field at the cathode surface and the increase of magnetic field with frequency in the interaction region. Consequently, one expects the noise figure to rise. Thus for a higher-frequency CWESA sample (variant 2) the value of the magnetic field ratio does not exceed the level of 7.8. In this case the value of would be greater than 1.45-1.50. For practical applications, the level of the noise temperature of an input amplifier over the operational frequency band is usually more important than the minimal value in at particular frequency point. Using the technique of optimizing the complex-conjugate matching of conductivities (see sections 3.2 and 3.4) makes it possible to broaden considerably the CWESA operational frequency band at the expense of some increase in general level of the noise factor.

The results of measurements of noise temperature of the CWESA samples over the operational frequency band are given in Fig.(6.6). Comparison of the noise temperature dependencies for tested CWESA samples with the variations in VSWR for input couplers confirms the conclusion of direct influence of the complex-conjugate matching of conductivities on the CWESA bandwidth. In the case of equal gaps in the input and output CWESA couplers (0.27 mm for variant 1) it is possible to increase considerably their load by the electron beam:

$$G_L + G_C = 0.71G_o \qquad (6.6)$$

and to provide compensation of the reactive component of the conductivity over the operational frequency band.

In this case the minimum value of the noise temperature (below the level of 120° K) is realized at two frequencies that are symmetrical with respect to the central frequency of the band, while the noise bandwidth at the level 140° K reaches 11%. A slight excess of the minimal level of measured values of the noise temperature as compared with the value of calculated in accordance with Eq.(6.5) can be considered to be due to the influence of non-uniform electric fields in the electron gun region.

For the higher frequency CWESA sample (variant 2) the gap between the coupler pads is 0.18 mm and the load by the beam is somewhat smaller at the beam current value of 250 μA :

$$G_L + G_C = 0.79G_0 \qquad (6.7)$$

In this case the operational frequency bandwidth at the level of 200K is as high as 6%, whereas the relative variation in over operational band is found to be slightly smaller as compared with that of variant 1. The transit angle for the resonator is about 83.1 radian and it provides quite adequate compensation of over the operational frequency band. However, a relative smaller magnetic field ratio (n = 7.8) causes the minimal values of to increase up to 160K.

D. CWESA Dynamic Range

Section 4.C presented the analysis of reasons for limitation of the CWESA dynamic range: 1) beam interception in the output resonator; 2) dynamic deceleration of the electron beam in the process of electrostatic amplification; and 3) excitation of longitudinal velocity spread in the electron beam during the gain. As noted above, the gap between the pads of the output coupler in CWESA samples was reduced to increase its load by the electron beam and to broaden the operational frequency bandwidth. In addition, gain was limited at the level of 10-12 dB. Under these conditions the CWESA dynamic range is determined by the electron beam interception in the output coupler.

Results of signal power transmission measurements in the CWESA as a function of input signal power for two samples (1 and 2) are represented in Fig. (6.7). In the absence of amplification ($V_0 = 0$) the signal losses do not exceed 0.5-0.8 dB up to ≈50 W. With gain of about 10 dB ($V_0 = 41$ V and $V_0 = 21$ V for variants 1 and 2, respectively) the electron beam interception in the output coupler becomes noticeable at power greater than 10 μW. A further increase in the input signal power leads to increasing beam interception and reducing gain.

For numerical estimation of the CWESA dynamic range, it is necessary to take into account the expansion of the electron beam in the adiabatically divergent magnetic field of the drift region, the level of beam radius pulsation, spread of specification limits on non-coaxiality of the device and a number of other factors leading to increase of the beam cross-section. As a result, beam interception can begin at > 14 μW for variant 1, and at > 29 μW for variant 2, which is consistent with the measurement data.

It should once again be pointed out that the measured level of the dynamic range is not the limiting one for CWESA's but rather is a result of certain compromises for

optimization of the whole complex of CWESA output characteristics. Note that it is possible to increase the CWESA dynamic range by additional +20 dB by electronic control of the potentials of the gain structure (decrease down to zero) and couplers (increase) in accordance with rise of input signal power. Moreover, the transistor amplifier placed directly in the CWESA package increases the total gain of the combined CWESA up to 20-25 dB.

Figure (6.8) illustrates two-tone intermodulation distortion for such combined CWESA when two signals within the pass band and are being amplified. For this device, the gain (CWESA + transistor stage) is approximately 23.5 dB. The measured value of the third-order intercept point is typical for CWESA and equals 18 dBm, whereas the power levels of the combined components ($2\omega_1-\omega_2$ and $2\omega_2-\omega_1$) at the 1-dB compression point do not exceed -16 dBm. Thus, the CWESA plus transistor amplifier linearity is approximately the same as for low-noise transistor amplifiers, and may even by dominated by the transistor amplifier.

A further increase in the input signal power will result in complete electron beam interception in the input coupler and activation of the CWESA self-protection mechanism against powerful microwave overload. Measurement results for VSWR for the input coupler without the electron beam and with full loading by the beam clearly illustrate the action of this self-protection mechanism, Fig. (6.9). In the case of complete transition of the electron beam through the coupler the measured values of VSWR over the operational frequency band are found to be smaller than 2.0. In the absence of the electron beam the value of the VSWR exceeds the level of 30.0 over the entire frequency band. This corresponds to practically complete reflection of the input power from the CWESA input coupler.

In the case of a powerful (up to 500 kW) square-pulse input supplied at the CWESA input, the action of the CWESA self-protection mechanism is illustrated by Fig. (6.10). The power of microwave the oscillations inside the input resonant cavity is determined by the level of VSWR in the case of complete beam interception (about 30) and can amount only to a few percent of the pulse power supplied at the CWESA input. With the end of input pulse, microwave oscillations in the input coupler are attenuated in accordance with the value of loaded quality factor Q_L.

The power level of oscillations inside the output resonant cavity during the high power pulse is determined by the isolation between the CWESA input and output (up to 120 dB). At the moment when the power of the oscillations inside the input cavity reaches the dynamic range limit (of the order of 10^{-4}W), the conditions for the electron beam transition through the gain structure and the output resonator are restored. The corresponding transit time of the beam is quite short, a few nsec. With restoration of the beam transition to the CWESA collector, the level of microwave oscillations in the output resonator practically is changed in accordance with the law of oscillation power variation in the input cavity. The necessary time of recovery of full serviceability of

the CWESA (the maximum sensitivity) after termination of the powerful microwave impact depends on the input power level and may be shorter than 10-20 ns.

E. The Millimeter Wave Receiver Protectors.

While millimeter wave CWESA's and CWPA's have not yet been developed, ISTOK has developed receiver protectors at both K_u and K_a band. These are simply the input and output coupler stages of the CWESA (or CWPA) with no amplification stage between them. Since the input coupler reduces the fast cyclotron wave noise on the beam, and there is no coupling to the uncooled slow cyclotron wave in any stage (since there is no amplification), this is a low noise receiver protector. A summary of the parameters of these millimeter wave receiver protectors is given in Table 6.2.

Table 6.2
ISTOK Cyclotron Wave Receiver Protectors

Frequency GHz	19	35
Bandwidth %	6	2.2
Allowed overload, pulsed kW	10	not tested
Allowed overload, steady state kW	0.5	0.02
Insertion loss db	0.5	0.5
Protection of subsequent stages db	70	52
Recovery time nsec	10	10

It should be emphasized that these results are preliminary at this point; it is very likely that all of these specifications could be considerably improved with little development.

VII Tests of the CWESA at the Georgia Tech Research Institute (GTRI)

GTRI has purchased X-Band ESCA's from ISTOK for use in an experimental high power pulsed Doppler radar. The pulse repetition rates vary from less than 1 kHz to several hundred kHz with pulse duration mainly down to less than 1 μs. Thus it is essential that the receiver recover as rapidly as possible after a microwave overload. If the receiver takes say 2 μsec before it is fully recovered, this could degrade the available time for data processing by 20%-50%. GTRI rejected conventional gas TR tubes as having both too long (order microseconds) and too unpredictable recovery time for the application. Prior to finding out about the ESCA, the radar used receiver protectors based of multipactor discharges, which also have a very fast recovery time. However these had spike leakage of 1-10 Watts, so a varactor diode was also required in the receiver protector chain. The insertion loss of the multipactor was about 1-1.5 dB, and that of the varactor was about 0.5 dB. Also the multipactor tube cost typically $10-20k and its operation required the working of many additional systems such as an oxygen generator, an ion pump, an electron gun, and a cooling system, since the incident power is absorbed rather than reflected.

Upon learning of the ESCA during a 1992 during a trip to Moscow (this work was also presented at the 1993 IEEE Microwave Conference in Atlanta[48]), it seemed to be a very attractive option. It combined in one package a low noise, very linear amplifier with an amplification in excess of 20dB, a large dynamic range which could be electronically controlled, as well as a reflecting (ie no need for cooling) receiver protector with less than a 50 nsec recovery time. Due to the continually increasing cost and delivery times of multipactor devices, the ESCA's appeared to be an attractive option, and GTRI evaluated and purchased several ESCA's for use in its radar system. Prior to insertion in the system, they were thoroughly tested, and some of the more interesting tests are described below.

One of the first, and most fundamental tests is a measurement of the amplification as a function of frequency. Shown in Fig.(7.1) is the output power as a function of frequency for an input power of -30 dBm. The bandwidth matches the ±1 dB value of 200 MHz as specified for the unit. The value of gain as a function of input power is shown in Fig. (7.2). The device is exceedingly linear up to -20 dBm as shown. The 1 dB compression point (the power at which the gain is 1dB less than the linear gain) is at an input power of -13dBm, or 50μW. Actually the dynamic range, as defined by the 1 dB compression point varied slightly as a function of frequency within the band. All of the GTRI data showed the 1 dB compression points corresponding to an input power of between -20dBm and -13 dBm. From there to about 10 milliwatts, the device behaves essentially as a saturated amplifier. Slightly above 10dBm, the receiver protection aspect becomes activated. The output power immediately drops to about -50 dBm. Thereafter, it slowly creeps back up. This increase is almost certainly the leakage of the power through various unintended pathways (backdoor coupling in the microwave directed energy HPM parlance), and no attempts were made to reduce this in the experimental equipment. Undoubtedly the device can be optimized to further reduce this leakage.

However the protection against the transmitter radar pulse is actually much greater. The CWESA used was actually a two stage amplifier within the container; the first amplifier is a CWESA, and the second is a standard transistor amplifier. Each stage provides roughly 10 dB of amplification. Since the timing of the radar transmitter pulse is well known, a blanking pulse can be applied to the transistor amplifier to further reduce the gain. This was accomplished by removing the power supply voltage from the transistor amplifier for the duration of the transmitted pulse. When a blanking pulse is used, the isolation through theESCA is greater than 90 dB and exceeded the measurement limit of the equipment.

The upper end of dynamic range of the ESCA is shown in Fig (7.2), this upper limit may be considerably extended by controlling the voltages, and especially V_o (see Fig. 6.2). This can be done very quickly, with a typical lower limit of a few microseconds set by the time for the electrode voltages of the ESCA to stabilize. Typically the tubes, as manufactured by ISTOK have two voltage settings so as to provide for electronic control of the dynamic range by mens of a 10 dB gain reduction. GTRI desired additional dynamic range, so the CWESA's were specially made with four voltage settings corresponding to gain reductions of 0, 10, 20, and 30 dB. The amplification as a function of frequency and voltage setting are shown in Fig.(6.3). As long as the output power is below about 10 mW, the amplification is linear at each voltage setting. The noise figures for conditions 1 and 2 are respectively 3.7 and 4 dB. The noise figures for conditions 3 and 4 were not measured, but were undoubtedly much higher. However when used in these conditions, the GTRI radar was looking at very large cross section targets, so there was no need for low noise temperature in the receiver.

Another important consideration is the linearity of the tube as reflected in third order intermodulations components. If there are two frequencies, ω_1 and ω_2 simultaneously incident on the ESCA, a nonlinear effect mixes the two and produces a third at for instance $2\omega_1-\omega_2$. Since the radar may interpret this as a third signal, or an additional velocity in a Doppler radar, it is important that these intermodulations be very small. As discussed earlier, the fact that the beam displacement is transverse and there is no longitudinal bunching renders the interaction very linear in nature. The susceptibility of the CWESA to intermodulations was tested at GTRI by injecting two signals 1 MHz apart in frequency. Shown in Fig.(7.4) are output powers of the two equal amplitude signals third order and intemodulation product at three different power levels. Over these three tests, the average value of the third order intercept point referred to the output is 16.5 dBm. Thus the device is quite linear as regards third order intermodulations.

An important aspect of the ESCA for the GTRI application was the recovery time after a microwave overload. The recovery time has not been specifically measured in the system, but is a small fraction of the transmitted pulse width. This may be confirmed by an examination of the range Doppler display of the GTRI experimental radar reproduced in Fig. (7.5). The radar had a nominal clutter attenuation of 100 dB. This figure presents output amplitude which is color coded from low amplitude (dark) to high amplitude (light) for each of the range Doppler cells. There are 10 fixed range gates covering the

interval between transmitted pulses and 512 Doppler Bins covering the Doppler frequency range ±50 kHz, regardless of PRF. In this figure only ±25 kHz is displayed, and the region surrounding zero frequency clutter is blanked to eliminate distraction. The waveform which was transmitted was a nominal 1μs pulse at 100kHz PRF. The fact that there is no evident contamination in the first range bin immediately following the transmitted pulse indicates that the ESCA recovers rapidly and stably in less than 100 ns. In fact, test have indicated that this recovery time is dominated by the recovery time of the power supply blanking the transistor amplifier. The response time of only the CWESA portion is probably faster still. Furthermore, in this application,the ESCA operated in a system providing clutter attenuation on the order of 100 dB, with the maximum values limited by signal processing rather than the ESCA stability. Finally, several of the CWESA's have been operated well in excess of 2000 hours with no sign of performance degradation.

APPENDIX Kinetic Power of Transverse Waves

This appendix derives the kinetic power of transverse electrostatic beam waves[49]. It does so by evaluating the power input from an external electric field in setting up these waves. If a filamentary electron beam with the linear charge density q is placed in the transverse electric field $E_\perp = E_x + jE_y$, the power of energy exchange between the electric field and the electron beam element of the length dz is equal to:

$$dP_\perp = q \cdot (E_x V_x + E_y V_y) \cdot dz = q \cdot \mathrm{Re}(E_\perp V_\perp^*) \cdot dz, \qquad (A.1)$$

where $V_\perp = V_x + jV_y$, the sign * denotes the complex-conjugate value.

Besides interaction with the transverse electric field, it is necessary to take into account the interaction of the electric beam with a longitudinal electric field E_z. To determine the value of E_z, we use the quasi-stationary approximation $(\vec{\nabla} \times \vec{E} = 0)$ for which near the z axis:

$$E_z(x,y,z,t) = x\frac{\partial E_x}{\partial z} + y\frac{\partial E_y}{\partial z}, \qquad (A.2)$$

or

$$E_z(\zeta,z,t) = \mathrm{Re}\left(\zeta^* \frac{\partial E_\perp}{\partial z}\right), \text{ where } \zeta = x + jy. \qquad (A.3)$$

Accordingly, the power of energy exchange with the longitudinal field E_z has the form:

$$dP_z = q \cdot V_z \cdot E_z \cdot dz = qV_z \mathrm{Re}\left(\zeta^* \frac{\partial E_\perp}{\partial z}\right) dz. \qquad (A.4)$$

The expression for the transverse velocity can be given in the form:

$$V_\perp = V_x + jV_y = \frac{\partial \zeta}{\partial t} + V_z \frac{\partial \zeta}{\partial z} = V_s + V_z \frac{\partial \zeta}{\partial z}, \qquad (A.5)$$

where V_s means the transverse velocity of the electron beam trace in the plane $z = \mathrm{const}$.

Summing up the powers of the longitudinal and transverse energy exchanges, we can write:

$$dP = dP_\perp + dP_z = q\left[\mathrm{Re}(E_\perp V_s^*) + V_z \frac{\partial}{\partial z}\mathrm{Re}(E_\perp \zeta^*)\right] dz. \qquad (A.6)$$

Now, we can use the representations:

$$V_s(z,t) = V_{s+}(z)e^{j\omega t} + V_{s-}(z)e^{-j\omega t}, \qquad (A.7)$$

$$E_\perp(z,t) = E_+ \exp j\omega t + E_- \exp -j\omega t \qquad (A8)$$

$$\varsigma(z,t) = R_+(z)e^{j(\omega t-\varphi)} + R_-(z)e^{-j(\omega t-\varphi)}, \quad \varphi = \int_0^z \beta_e dz, \qquad (A.9)$$

and, accordingly:

$$V_{s+}(z) = j\omega R_+(z)e^{-j\varphi}, \; V_{s-}(z) = -j\omega R_-(z)e^{j\varphi}. \qquad (A.10)$$

Substituting (A.7)- (A.10) into (A.6) and averaging the power over the period $2\pi/\omega$, we get:

$$dP = q\left[\mathrm{Re}(E_+ V_{s+}^*) + \mathrm{Re}(E_- V_{s-}^*) + V_z \frac{\partial}{\partial z}\{2\,\mathrm{Re}(E_+ R_+^* e^{j\varphi} + E_-^* R_- e^{-j\varphi})\}\right]dz. \qquad (A.11)$$

Integrating (A.11) over z from 0 to z, and taking into account that $I_b = -q(z)V_z(z)$, we find:

$$P = P_+ + P_- + \Delta P, \qquad (A.12)$$

$$P_\pm = -I_b \int_o^z \mathrm{Re}(E_\pm V_{s\pm}^*)\frac{dz}{V_z}, \qquad (A.13)$$

$$\Delta P = -I_b \int_o^z d\{2\,\mathrm{Re}(E_+ R_+^* e^{j\varphi} + E_-^* R_- e^{-j\varphi})\}. \qquad (A.14)$$

The expression between the braces under sing of integral depends only on the coordinate z, therefore the following substitution was used: $d/dz\{\,\} \rightarrow \partial/\partial z\{\,\}$.

Now, choosing the integration limits outside (before and after) the interaction region, i.e. where the transverse electric field is equal to zero ($E_\pm(0) = E_\pm(z) = 0$), we have:

$$\begin{aligned} P &= P_+ + P_-, \\ \Delta P &= 0. \end{aligned} \qquad (A.15)$$

Let us first consider the simplest case:

$$\omega_c = \mathrm{const}, \; V_z = V_z(z). \qquad (A.16)$$

Then the equations for transverse wave amplitudes have the form:

$$\frac{dR_{1\pm}(z)}{dz} = j\frac{eE_{\pm}}{m\omega_c v_z} e^{j(\pm\varphi-\psi)}, \qquad (A.17)$$

$$\frac{dR_{2\pm}(z)}{dz} = -j\frac{eE_{\pm}}{m\omega_{co} v_z} e^{\pm j\varphi}; \quad \varphi = \int_0^z \beta_e\, dz, \psi = \int_0^z \beta_c\, dz\,. \qquad (A.18)$$

Besides:

$$\begin{aligned} \varsigma(z,t) = {} & R_{1+}(z) e^{j[\omega t - \int_0^z (\beta_e - \beta_c) dz]} + R_{1-}(z) e^{-j[\omega t - \int_0^z (\beta_e + \beta_c) dz]} \\ & + R_{2+}(z) e^{j(\omega t - \int_0^z \beta_e\, dz)} + R_{2-}(z) e^{-j(\omega t - \int_0^z \beta_e\, dz)}\,. \end{aligned} \qquad (A.19)$$

We find $E_{\pm}$ from (A.17), (A.18), substitute them into the expression for energy exchange power (A.13) and take into account that:

$$V_{s+} = +j\omega R_+(z) e^{-j\varphi} = j\omega [R_{2+}(z) + R_{1+}(z) e^{j\psi}] e^{-j\varphi}, \qquad (A.20)$$

$$V_{s-} = -j\omega R_-(z) e^{j\varphi} = -j\omega [R_{2-}(z) + R_{1-}(z) e^{j\psi}] e^{j\varphi} \qquad (A.21)$$

Then assuming that the electron beam has no modulation at the input into the interaction region (i.e. $R_{1\pm}(0) = R_{2\pm}(0) = 0$) we finally get:

$$P_{\pm}(z) = P_{1\pm}(z) + P_{2\pm}(z) = (mI_o/2e)\omega_c\omega\{\pm |R_{1\pm}|^2 - \pm |R_{2\pm}|^2\}, \qquad (A.22)$$

or

$$P_{1\pm} = \pm I_o U_o \beta_e \beta_c |R_{1\pm}|^2 \qquad (A23a)$$

$$P_{2\pm} = -\pm I_o U_o \beta_e \beta_c |R_{2\pm}|^2 \qquad (A23b)$$

where U_o is the potential of the electron beam. The positive sign means that power is added to the electron beam to set up the wave, whereas the negative sign means that power is taken from the electron beam to set up the wave.

Acknowledgment

The authors would like to thank Herbert Leupold of the Army Research Laboratory, Drew Hazelton, Pradeep Haldar, Roger Wheatley, and Michael Parizh of Intermagnetics General Corporation, and Vilhelm Gregors-Hansen of NRL for a number of very useful discussions. This work was supported by the United States Office of Naval Research.

References

1. Cuccia C.L.: The Electron Coupler - a Developmental Tube for Amplitude Modulation and Power Control at UHF, RCA Rev., vol. 10, N 2, p. 270, 1949.

2. Adler R.: Parametric Amplification of the Fast Electron Wave, Proc. IRE, vol. 46, N 6, p. 1300, 1958.

3. Adler R., Hrbek G. and Wade G.: A Low-Noise Electron-Beam Amplifier, Proc. IRE, vol. 46, N 10, p. 1756, 1958.

4. Cuccia C.L.: Parametric Amplification, Power Control and Frequency Multiplication at Microwave Frequencies Using Cyclotron-Frequency Devices, RCA Rev., vol. 21, N2, p. 228, 1960.

5. Adler R. and Wade G.: Beam Refrigeration by Means of Large Magnetic Fields, J. Appl. Phys., vol. 31, N 7, p.1201, 1960.

6. Siegman A.E.: The DC-Pumped Quadrupole Amplifier - a Wave Analysis, Proc. IRE, vol. 48, N 10, p. 1750, 1960.

7. R. Gould and C. Johnson, Coupled Mode Theory of Electron Beam Parametric Amplifiers, J. Appl. Phys. 32, 248, 1961

8. Louisell W.H.: "Coupled Mode and Parametric Electronics," John Wiley & Sons, Inc., New York, London, 1960.

9. E.I. Gordon, Noise in Beam Type Parametric Amplifiers, Proc. IRE, 49, 1208, 1961

10. P.A.H. Hart, On Cyclotron Wave Noise Reduction, Proc. IRE, 50, 227, 1962

11. R. Adler, G. Hrbek, and G. Wade, The Quadrupole Amplifier, a Low Noise Parametric Device, Proc. IRE 47, 1713, 1959

12. Vanke V.A., Grigorenko L.P. and Magalinsky V.B.: Investigation of Amplitude-Phase Characteristics of Quadrupole Region of Electron-Beam Parametric Amplifier, Radiotekhnika i Elektronika, vol. 10, N 12, p. 2187, 1965

13. Vanke V.A. and Magalinsky V.B.: Statistical Properties of Output Signal of Quasi-Degenerative Electron-Beam Parametric Amplifier, Radiotekhnika i Elektronika, vol. 11, N 7, p. 1210, 1966

14. Lopukhin V.M., Magalinsky V.B., Martynov V.P. and Roshal A.S.: "Noises and Parametric Phenomena in Electron Beams," Nauka, Moscow, 1966

15. Lopukhin V.M. and Roshal A.S.: "Electron-Beam Parametric Amplifiers," Sov. Radio, Moscow, 1968

16. Vanke V.A., Lopukhin V.M. and Savvin V.L.: Super Low-Noise Cyclotron-Wave Amplifiers, Uspekhi Fizicheskikh Nauk, vol. 99, N 4, p. 545, 1969

17. Vanke V.A.: Interaction of Transverse Oscillations and Waves in the Electron Beams and Electromagnetic Fields, Doctor of Sciences (Phys. & Math.) Thesis, Faculty of Physics, Moscow State University, Moscow, pp. 1-430, 1979

18. Vanke V.A. and Savvin V.L.: On Some Microwave Physics Research at Moscow State University and Russian Industries (Plenary Talk), 23th IEEE Int. Conference on Plasma Science, Boston, June 3-5, 1996.

19. Kantyuk S.P. and Petrovsky V.B.: Characteristics of Resonant Coupler with Fast Cyclotron Wave of an Electron Beam in the Non-Uniform Magnetic Field, Elektronnaya Tekhnika, Ser. Elektronika SVCh, N 8, p. 29, 1982

20. Balyko A.K. and Petrovsky V.B.: Influence of Dismatched Load on the Bandwidth of Resonant Couplers, Elektronnaya Tekhnika, Ser. Elektronika SVCh, N 2, p. 64, 1988

21. This photo of the S300 PMU radar is taken from a brochure printed by the manufacturer, ALMAZ Scientific Industrial Corporation, 80 Leningradsky Prospect, Moscow, 125178, Russia

22. The fact that CWESA's are used as the input amplifier in the S300 PMU radar is taken from a brochure of Electronintorg Ltd. 24/2 Ulitsa Usievicha, Moscow, 125315, Russia

23. E.I. Gordon, A Transverse Field Traveling Wave Tube, Proc. IRE, 48, 1158, 1960

24. Hrbek G. and Adler R.: Low-Noise DC-Pumped Cyclotron-Wave Amplifier, Proc. of 5th Intern. Congress on Microwave Tubes (Paris, 1964), N.Y.-London, Acad. Press, p. 17, 1965.

25. Vanke V.A. and Savvin V.L.: Field Structure and Parameters Calculation of Quadrupole Spiral for Cyclotron-Wave Electrostatic Amplifier, Elektronnaya Tekhnika, Ser. Elektronika SVCh, N 12, p. 159, 1969

26. Vanke V.A. and Savvin V.L.: To the Theory of Amplification Processes in Cyclotron-Wave Electrostatic Amplifier, Radiotekhnika i Elektronika, vol. 15, N 11, p. 2317, 1970

27. Budzinsky Yu.A. and Kantyuk S.P.: Cyclotron-Wave Electrostatic Amplifiers, Elektronnaya Tekhnika, Ser. Elektronika SVCh, N 1, p. 21, 1993

28. Bykovsky S.V. and Vanke V.A.: Transverse Waves of an Electron Beam in the Quadrupole Electric Field, Radiotekhnika i Elektronika, vol. 40, N 8, p. 1277, 1995

29. Vanke V.A. and Magalinsky V.B.: On the Role of Space Charge at the Amplification of Intrinsic Noise Orbits in High-Frequency Quadrupole Field, Izvestiya VUZ'ov, ser. Radiofizika, vol. 9, N 5, p. 831, 1966

30. Bondarev A.S. and Kantyuk S.P.: Influence of Electron Deceleration in the Beams with Finite Density on the Dynamic Range of Cyclotron-Wave Electrostatic Amplifiers, in "Design of New Types of UHF Amplifiers," Kiev Polytech. Inst. Ed., Kiev, 1971

31. Bondarev A.S. and Kantyuk S.P.: Dynamic Dissynchronisation in Cyclotron-Wave Electrostatic Amplifiers with due Account of Space Charge Influence, Izvestiya VUZ'ov, ser. Radioelektronika, vol. 116, N 12, p. 30, 1973

32. R. Adler and A. Ashkin and E.I. Gordon, Excitation and Amplification of Cyclotron Waves and Thermal Orbits inthe Presence of Space Charge, J. Appl. Phys. 32, 672, 1961

33. Vanke V.A. and Savvin V.L.: Shaping of Magnetic Field in Near-Cathode Region of Cyclotron-Wave Electrostatic Amplifier, Elektronnaya Tekhnika, Ser. Elektronika SVCh, N 12, p. 143, 1969

34. Budzinsky Yu.A., Bykovsky S.V. and Murskov A.A.: Magnetic System of Electron-Vacuum UFH Device, Russian Fed. Patent 2024098, Appl. 08.01.91, BI N 22, 1994

35. Vanke V.A., Kryukov S.P. and Timofeev Yu.M.: On the Minimum Noise Level of Cyclotron-Wave Electrostatic Amplifier with Taped Electron Beam, Izvestiya VUZ'ov, ser. Radiofizika, vol. 14, N 1, p. 142, 1971 (in Russian).

36. Dudin Yu. N. and Kantyuk S.P.: Analysis of Cyclotron-Wave Electrostatic Amplifiers with Flatly-Symmetric Periodic System, Elektronnaya Tekhnika, Ser. Elektronika SVCh, N 4, p. 126, 1973 (in Russian).

37. Bykovsky S.V. and Vanke V.A.: Transverse Waves of an Electron Beam in Flatly-Symmetric Fields, Radiotekhnika i Elektronika, vol. 38, N 8, p. 1475, 1993

38. Vanke V.A. and Kryukov S.P.: Longitudinal Electron Velocity Spread and Gain Limitation in Cyclotron-Wave Electrostatic Amplifiers, Radiotekhnika i Elektronika, vol. 17, N 10, p. 2230, 1972

39. Vanke V.A. and Kryukov S.P.: Interaction of Cyclotron Waves of Multivelocity Electron Beam with Electrodynamics Systems, Izvestiya VUZ'ov, ser. Radiofizika, vol. 16, N 8, p. 1271, 1973

40. Vanke V.A., Kryukov S.P., Lopukhin V.M. and Zaitsev A.A.: On the Design of Narrow-Band Controlled Cyclotron-Wave Electrostatic Amplifier, Izvestiya VUZ'ov, ser. Radiofizika, vol. 15, N 2, p. 291, 1972

41. Vanke V.A., Lopukhin V.M. and Kantyuk S.P.: Analysis of Electron Double-Beam Parametric Amplifier, Radiotekhnika i Elektronika, vol. 14, N 4, p. 666, 1969

42. Drew Hazelton, Pradeep Haldar, Roger Wheatley, and Michael Parizh, Intermagnetics General Corporation, Latham, NY, private conversation, October, 1995

43. K. Halbach, Nucl. Instr. and Methods, 169, 1, 1980

44. K. Halbach, Nucl. Instr. and Methods, 187, 109, 1981

45. J. Coey and O. Cugat, Construction and Evaluation of Permanent Magnet Variable Flux sources, Proc. Int. Workshop on Rare Earth Permanent Magnets, September, 1995

46. H. Leopold and E. Potenziani, IEEE Trans. Magn. MAG 23, 3628, 1987

47. H. Leopold, A Tilak, and E. Potenziani, Doubly Augmented Magic Spheres, IEEE Trans. Magn. September, 1996

48. Budzinsky Yu.A. and Kantyuk S.P.: A New Class of Self-Protecting Low-Noise Microwave Amplifiers, Proc. IEEE MTT-S Microwave Symposium, Atlanta, USA, Digest vol. 2, p.1123, June 1993.

49. Bykovsky S.V. and Vanke V.A.: On Kinetic Power of Transverse Waves of an Electron Beam, Radiotekhnika i Elektronika, vol. 37, N 10, p. 1854, 1992

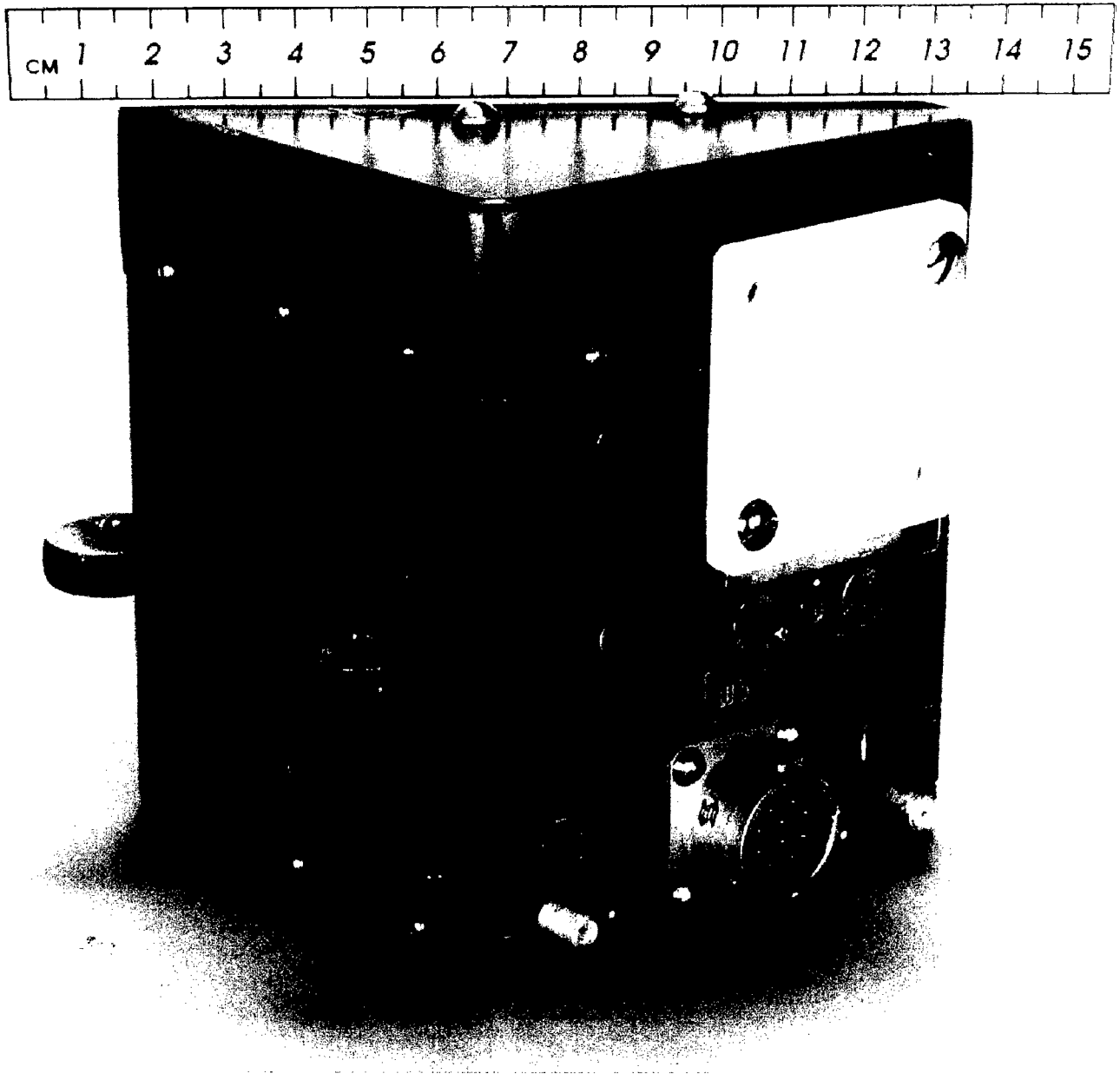

Figure 1.1 - The X-Band CWESA used in the Georgia Tech pulsed doppler radar.

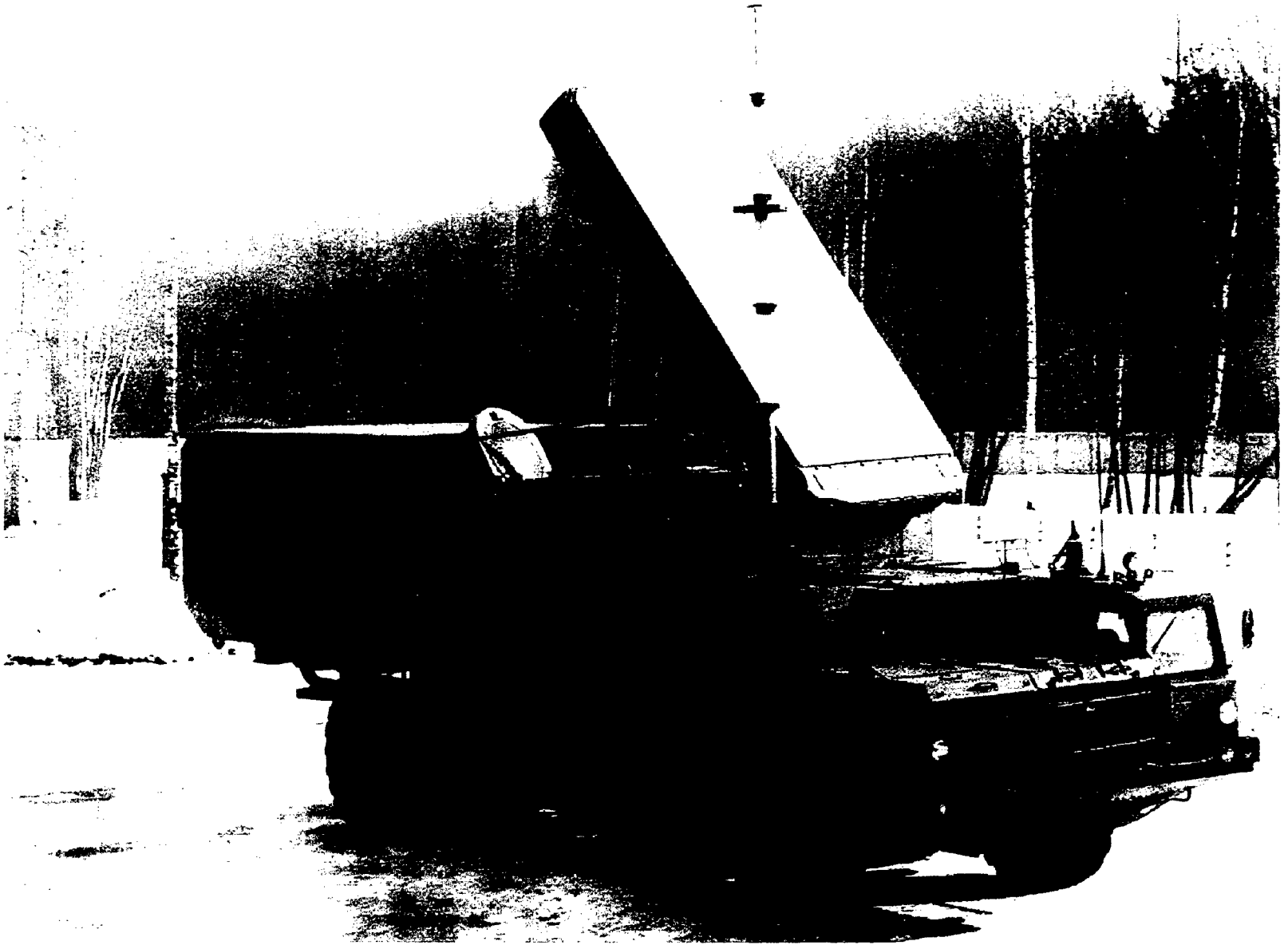

Figure 1.2 - The radar system for the Russian S300 mobile air defense system. This radar uses a cyclotron wave electrostatic amplifier for its receiver.

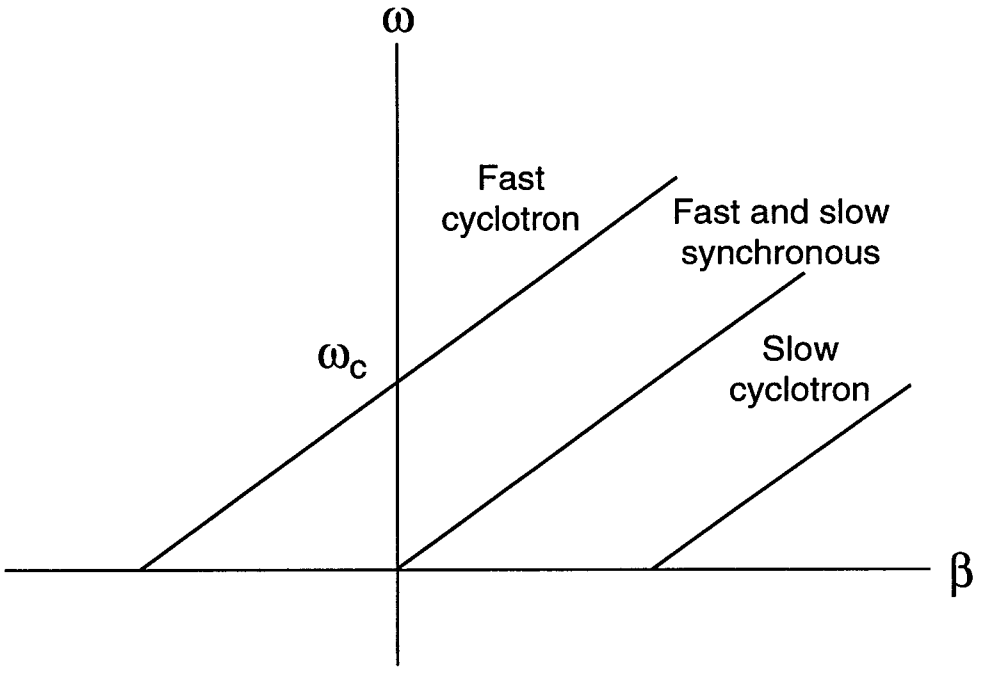

Fig. 2.1 - Dispersion relation for transverse beam modes
negelecting space charge.

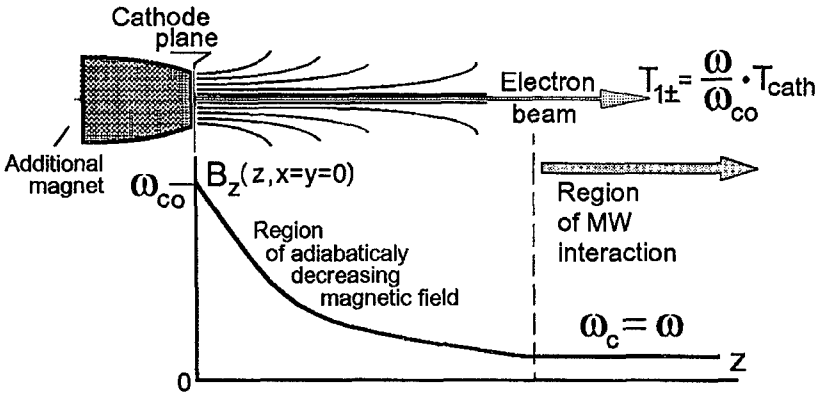

Fig. 3.1
General scheme of cyclotron wave noise reduction in the adiabatically decreasing magnetic field.

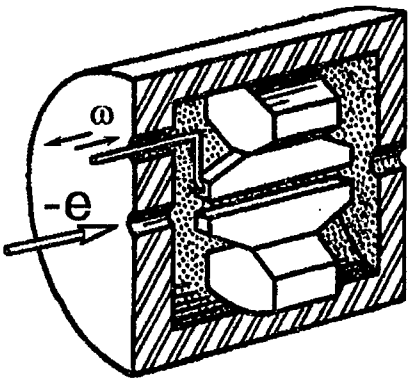

Fig 3.2a
Resonant coupler
with transverse electric field
in the interaction region .

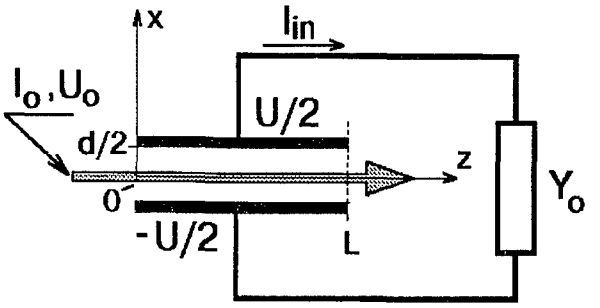

Fig. 3.2 b
Equivalent scheme
of resonant coupler.

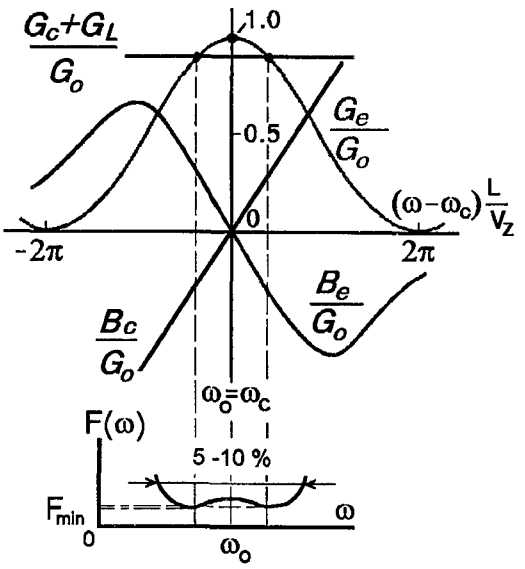

Fig. 3.3
Complex-conjugate matching of conductivities and the frequency
bandwidth of CWESA.

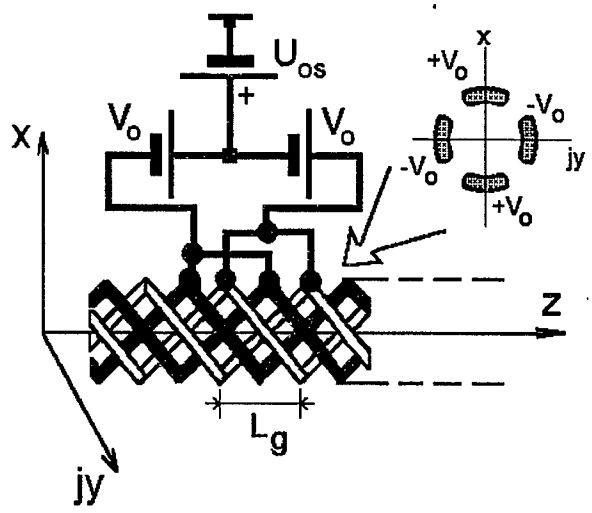

Fig. 4.1
Electrostatic gain structure
in the form of quadrupole spiral

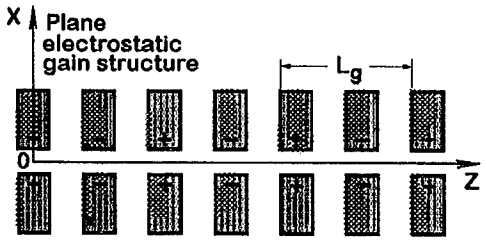

Fig. 4.2
Plane periodic gain structure.

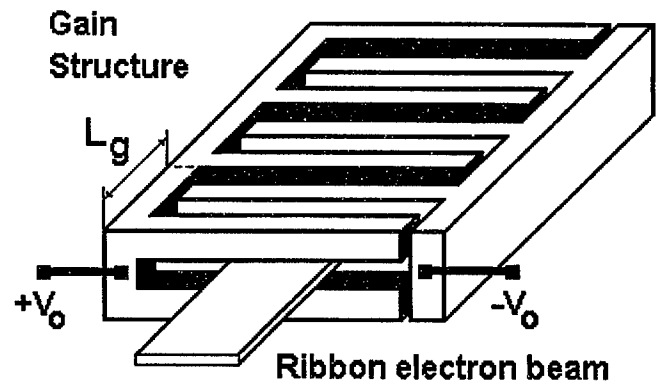

Fig. 4.3
The ribbon beam in the binary comb

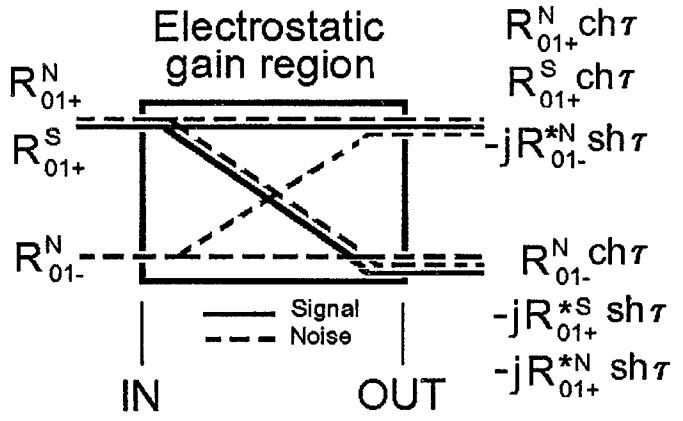

Fig. 4.4
Scheme illustrating the connection between the signal cyclotron waves and the noise cyclotron waves taking place in the process of electrostatic amplification.

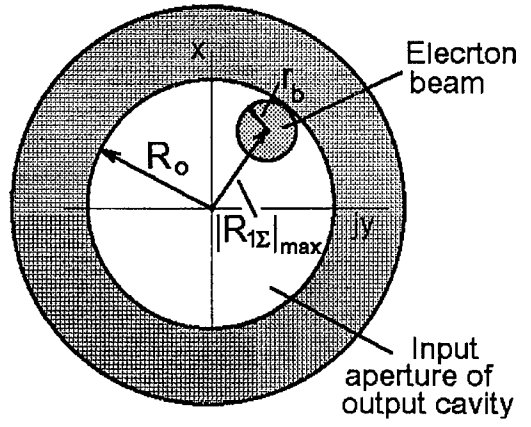

Fig. 4.5
Limitation of the fast cyclotron wave power in the input aperture of the output resonant cavity.

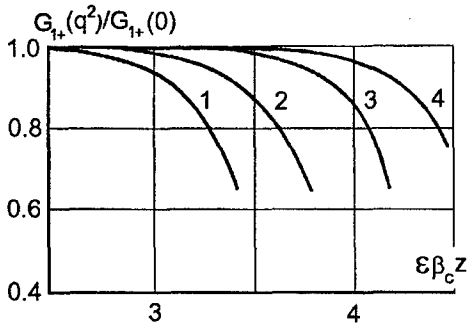

Fig 4.6

1 – $q^2 = 10^{-2}$; 2 – $q^2 = 5 \cdot 10^{-3}$;

3 – $q^2 = 2 \cdot 10^{-3}$; 4 – $q^2 = 10^{-3}$.

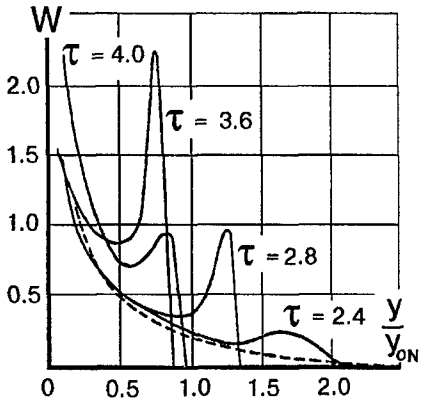

Fig 4.7

Computer simulation of the electron longitudinal velocity distribution for T_{cath} =1000°K, n=1, εU_{os} =9v

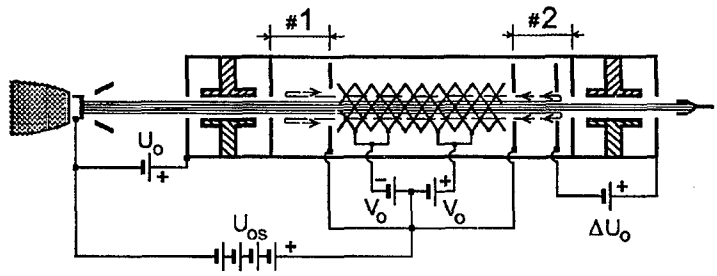

Fig. 4.8

Reflection of electrons in the transition regions of CWESA, when $U_{os} > U_o$. The additional potential ΔU_o realizes cut-off of slow electrons shunting the output resonator.

BEAM
INTERCEPTING

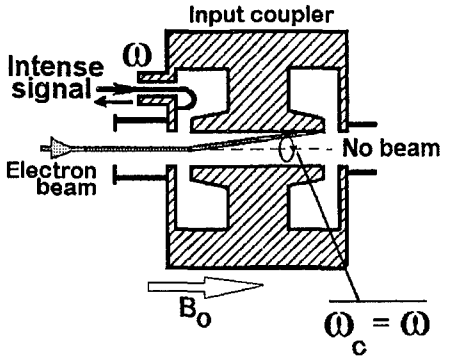

Fig.4.9
Input Cavity of the CWESA
as a receiver protector

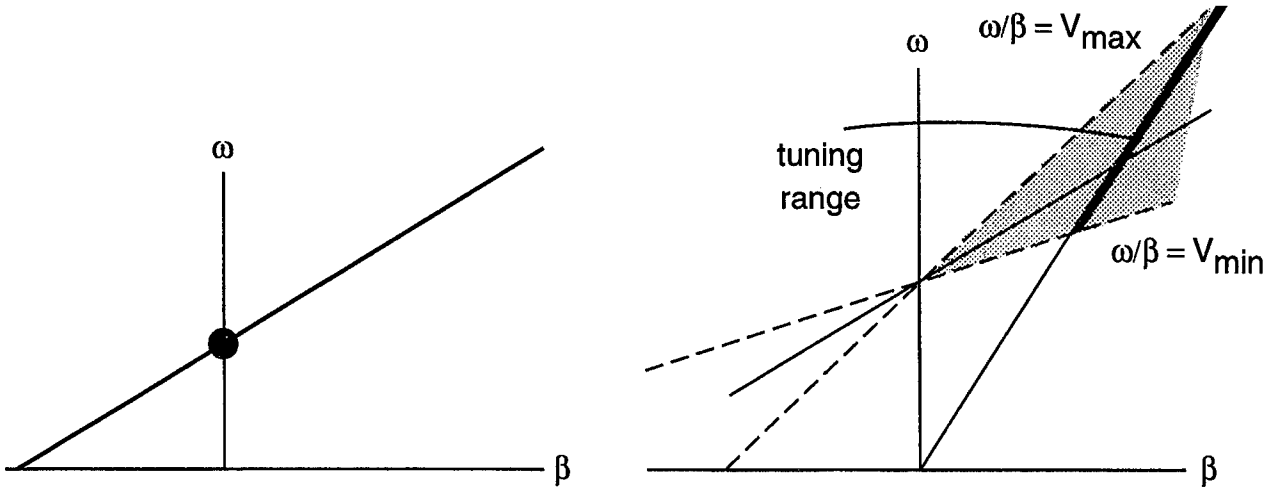

(a) Coupling of the fast cyclotron mode in a Cuccia coupler (the dot).

(b) Coupling of the cyclotron wave at different beam voltage to the tunable coupler.

Fig. 4.10

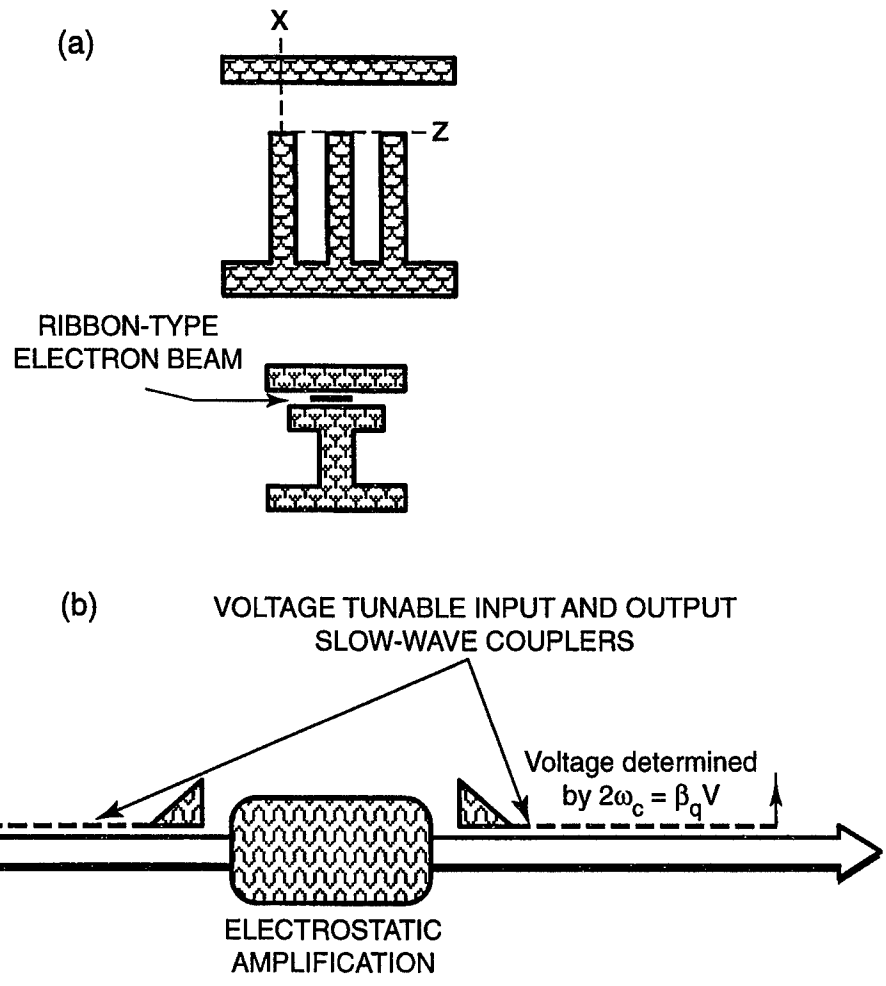

Fig. 4.11 - (a) The comb slow wave structure, (b) Schematic of the tunable CWESA. The voltage in the interaction region is determined by $2\omega_c = \beta_q V$.

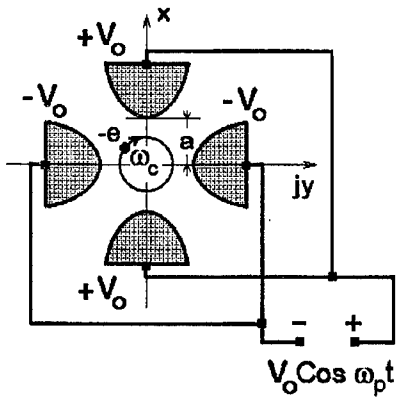

Fig 5.1
Scheme of parametric amplification
in the quadrupole field.

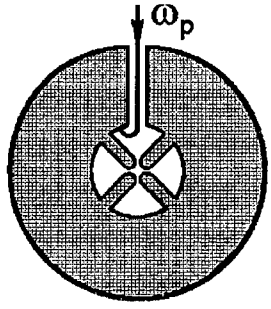

Fig. 5.2
Scheme of the
microwave
resonator with the
quadrupole field.

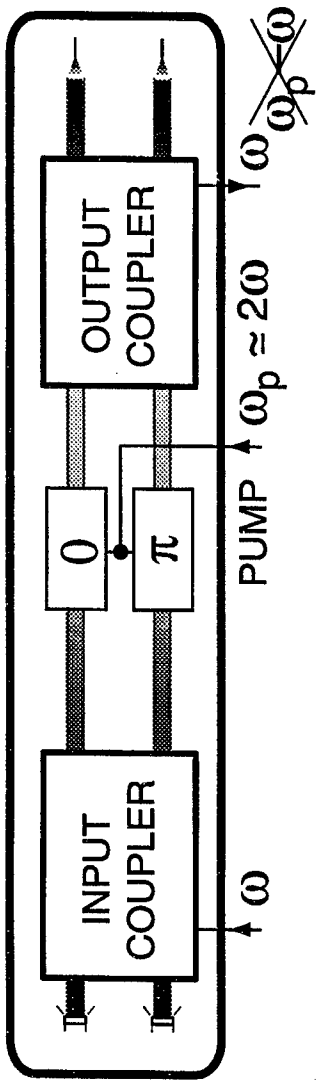

Fig. 5.3 - Two beam CWPA

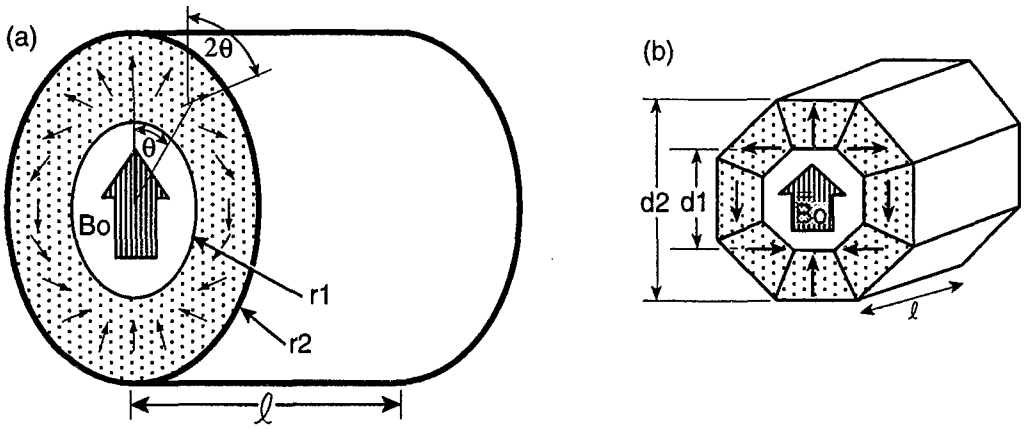

Fig. 5.4 - (a) An ideal Magic cylinder, (b) an octagonal approximation to it.

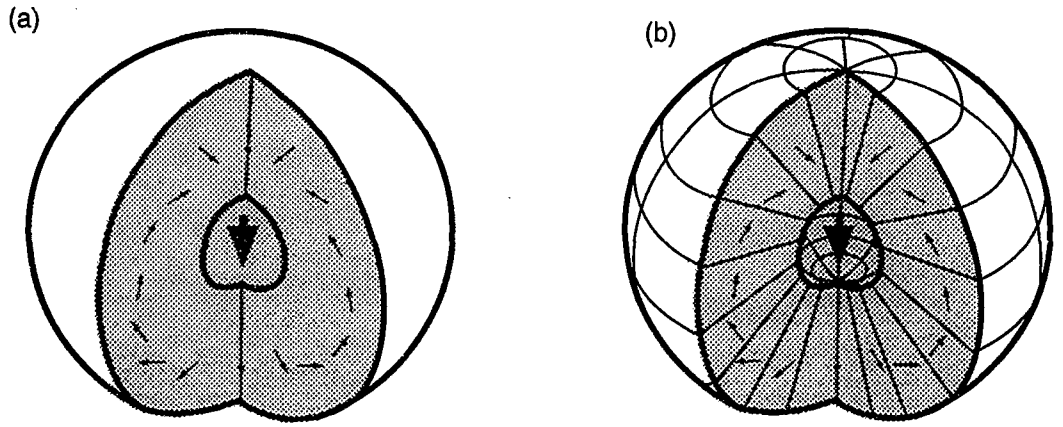

Fig. 5.5 - (a) An ideal and (b) a realizable magic sphere.

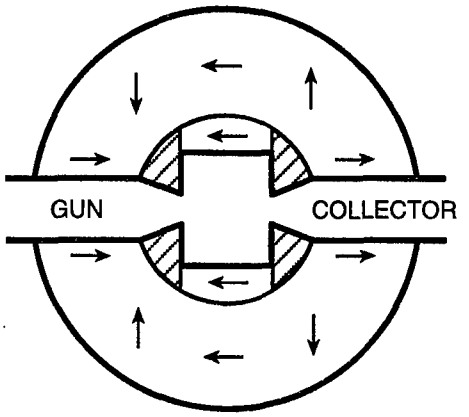

Fig. 5.6 - A microwave tube like the CWPA in an augmented magic sphere.

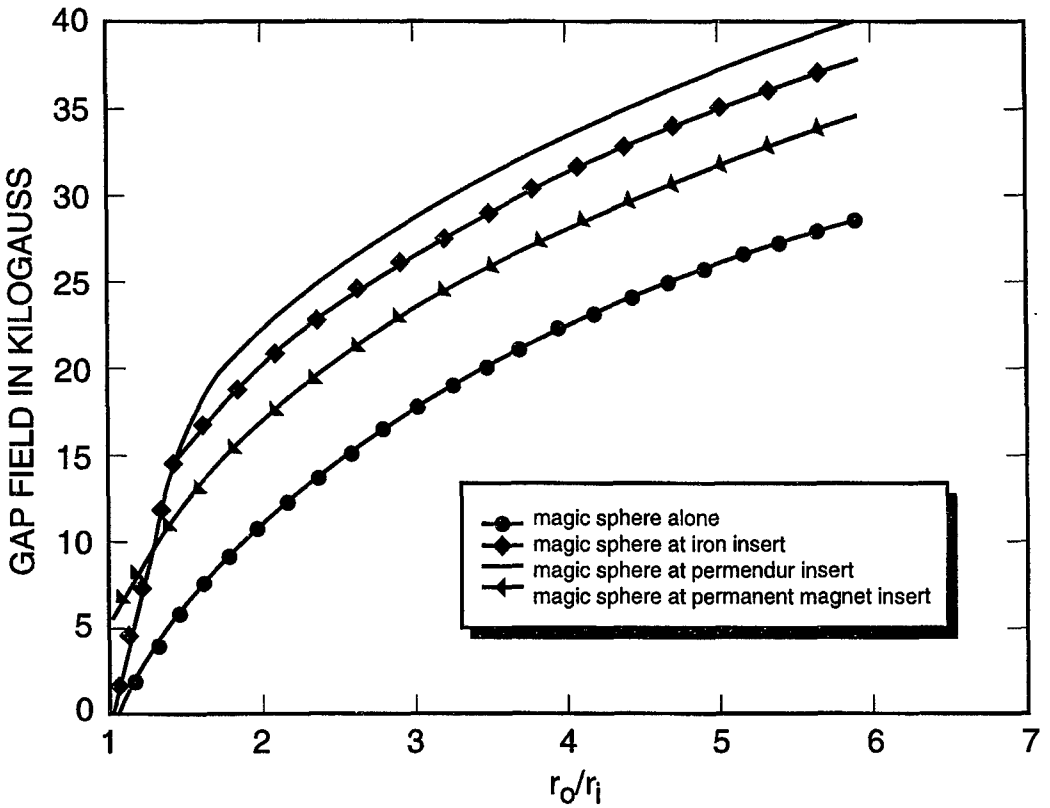

Fig. 5.7 - Gap fields for a variety of inserts within a magic sphere.

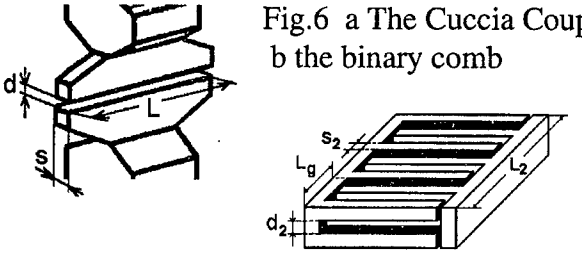

Fig.6 a The Cuccia Coupler
b the binary comb

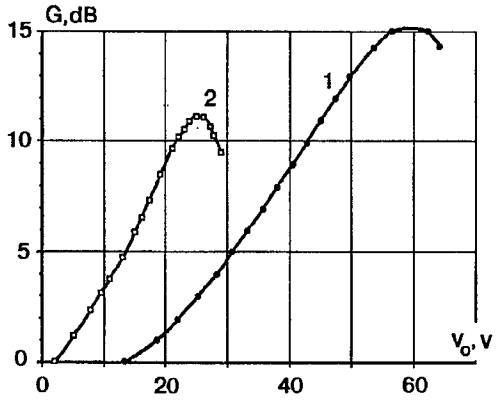

Fig.6.2 Gain as a function of V

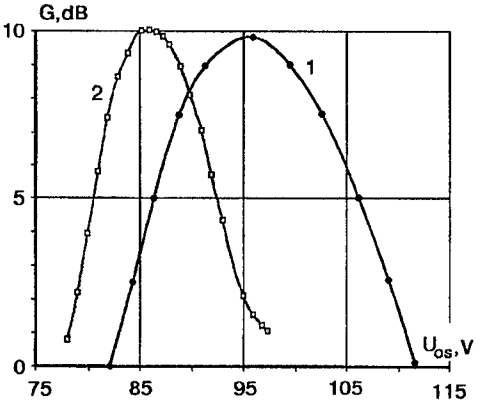

Fig 6.3 Gain as a function of U_{os}

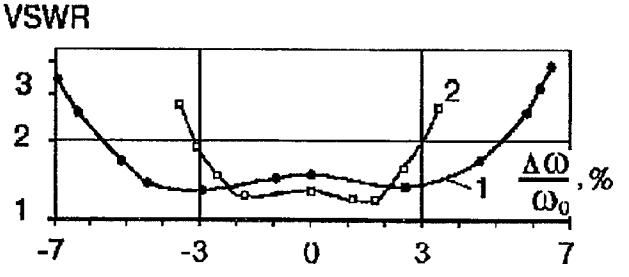

Fig. 6.4 The VSWR of the input coupler

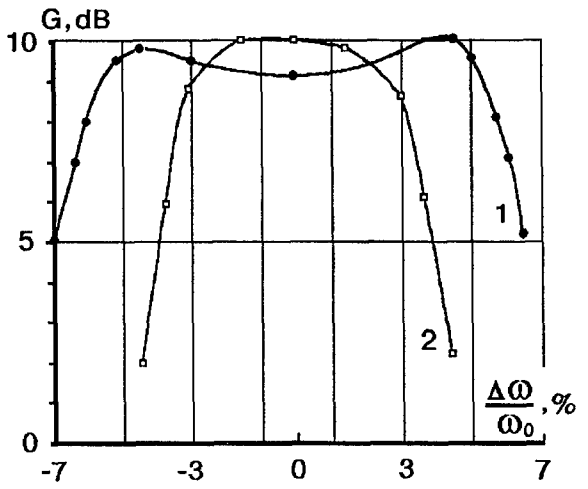

Fig 6.5 Frequency dependence of the gain

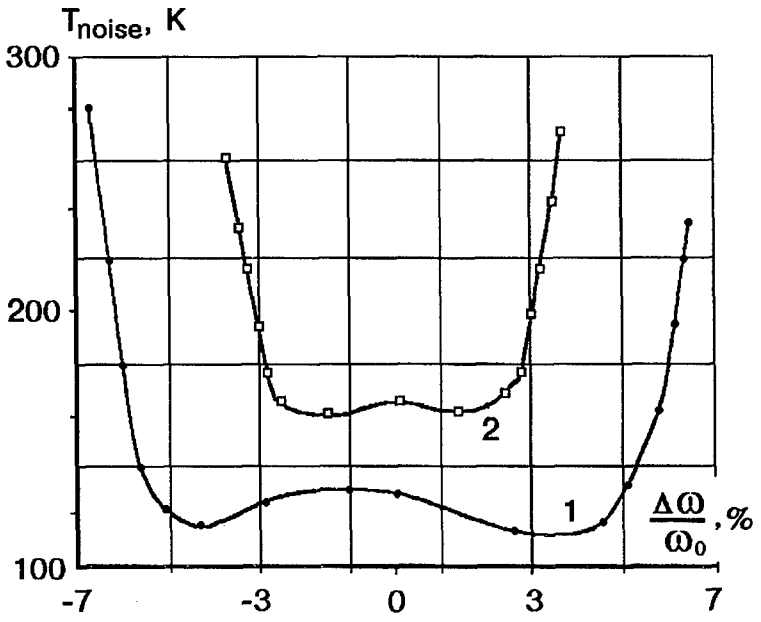

Fig. 6.6 The frequency dependence of the noise temperature

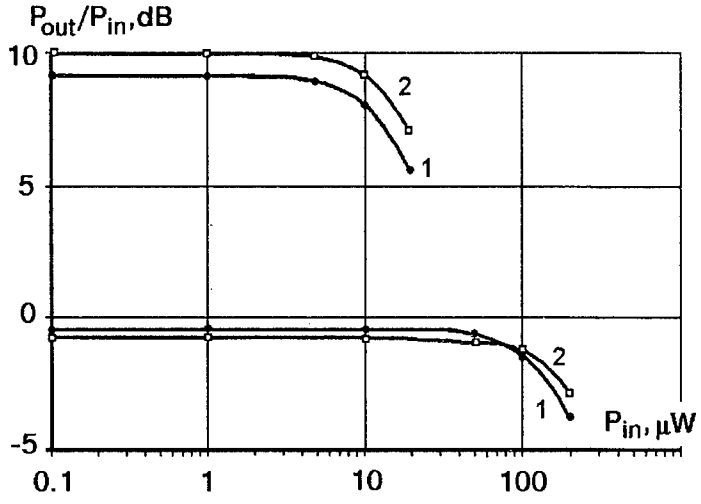

Fig 6.7 Dynamic Range and input loss of CWESA as a function of power

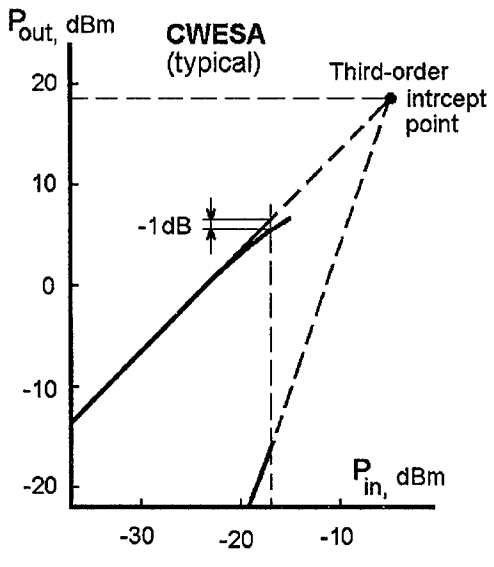

$G_{cwesa} + G_{ssa} \cong 23.5$ dB

Fig. 6.8 Intermodulation in the CWESA with the transistor amplifier booster

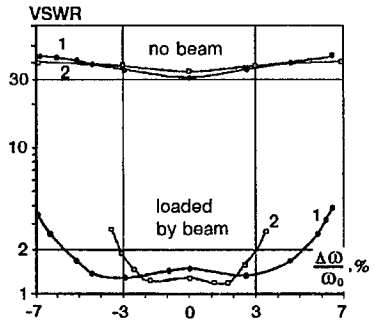

Fig 6.9 The CWESA acts as a receiver protector when the input signal exceeds that that for beam transmission

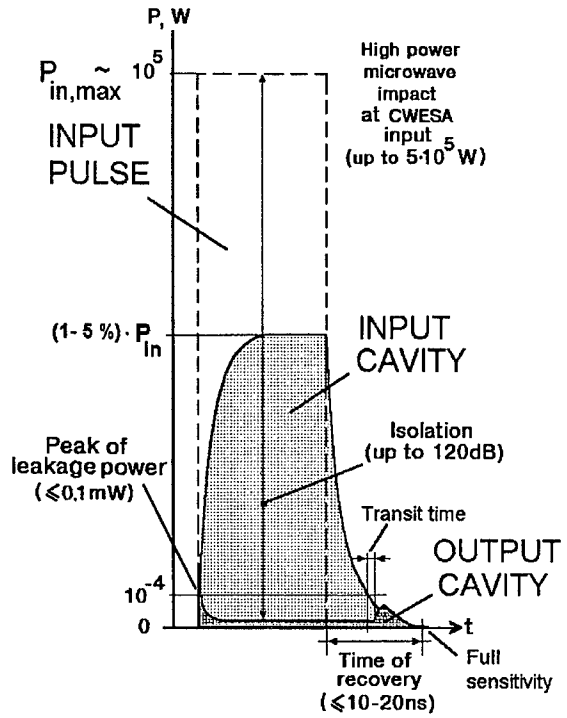

Fig. 6.10 The recovery of the CWESA from a microwave overload

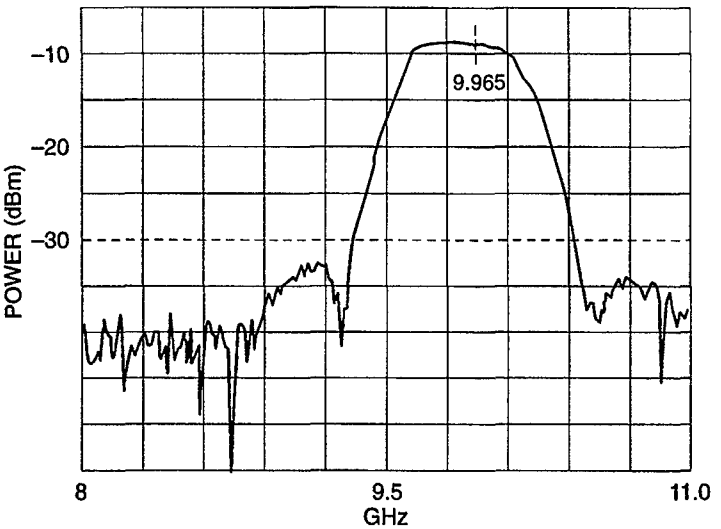

Fig. 7.1 - Linear gain of the CWESA.

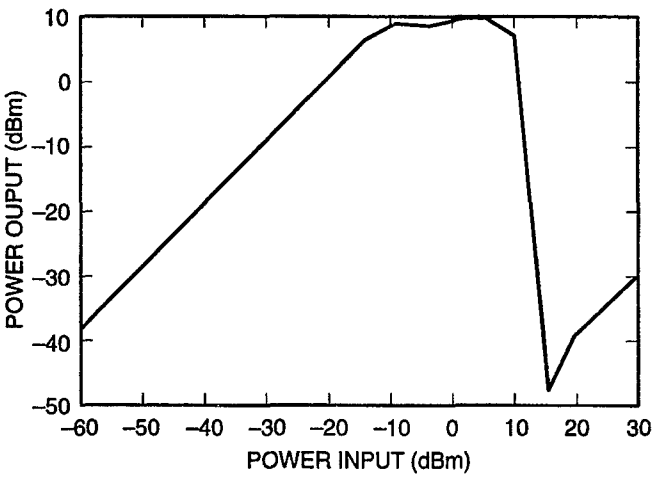

Fig. 7.2 - Transfer function of the ESCA, demonstrating the "self-protecting" behavior for high input signal levels.

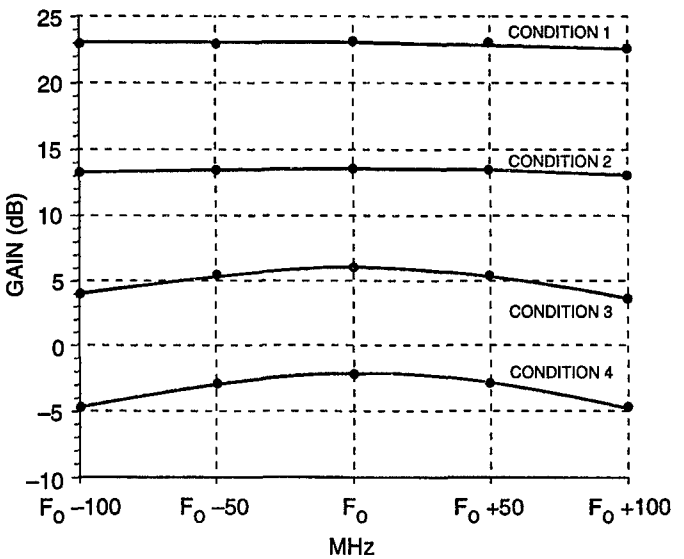

Fig. 7.3 - Electronic control of gain over a 200 MHz bandwidth.

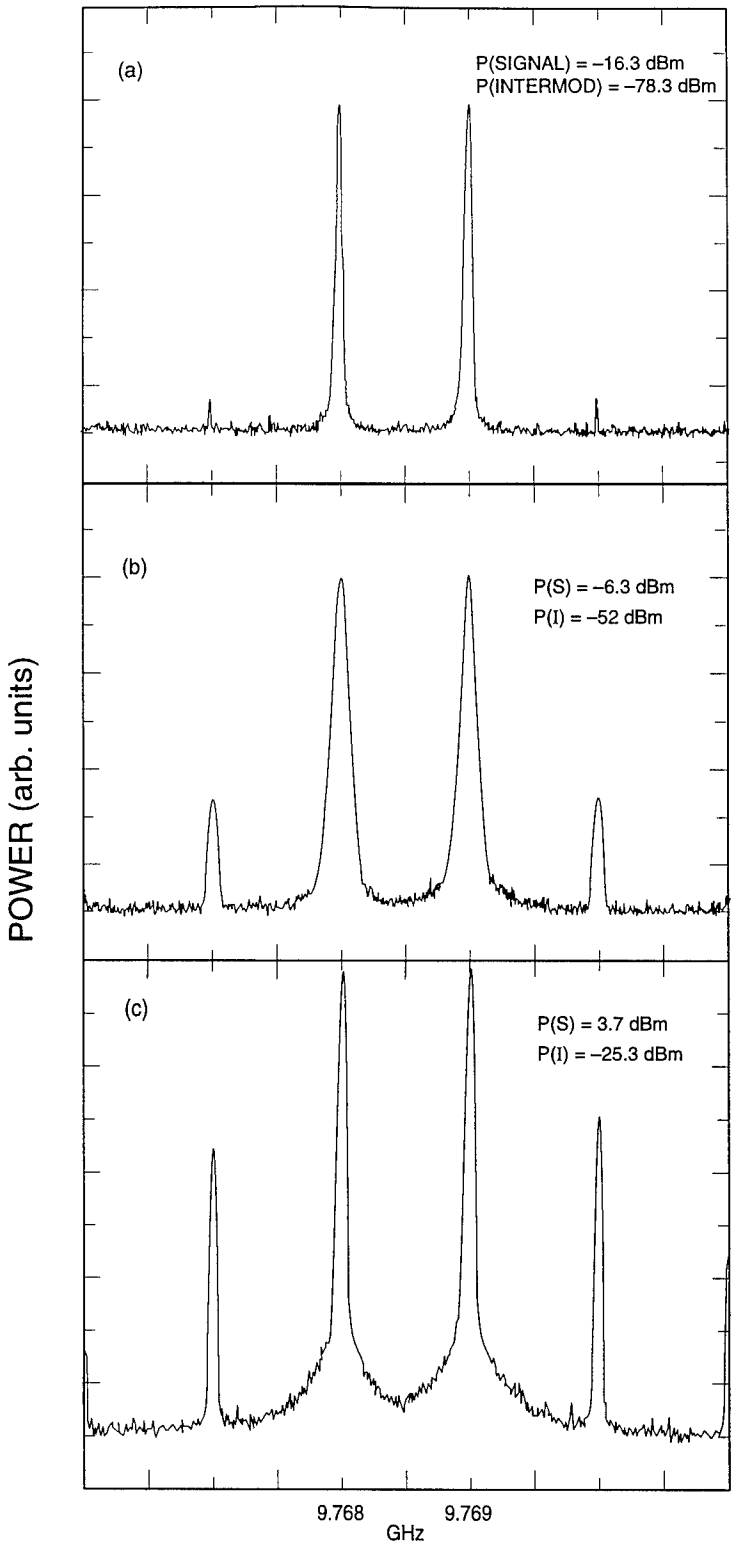

Fig. 7.4 - A test of the CWESA to third order intermodulation.

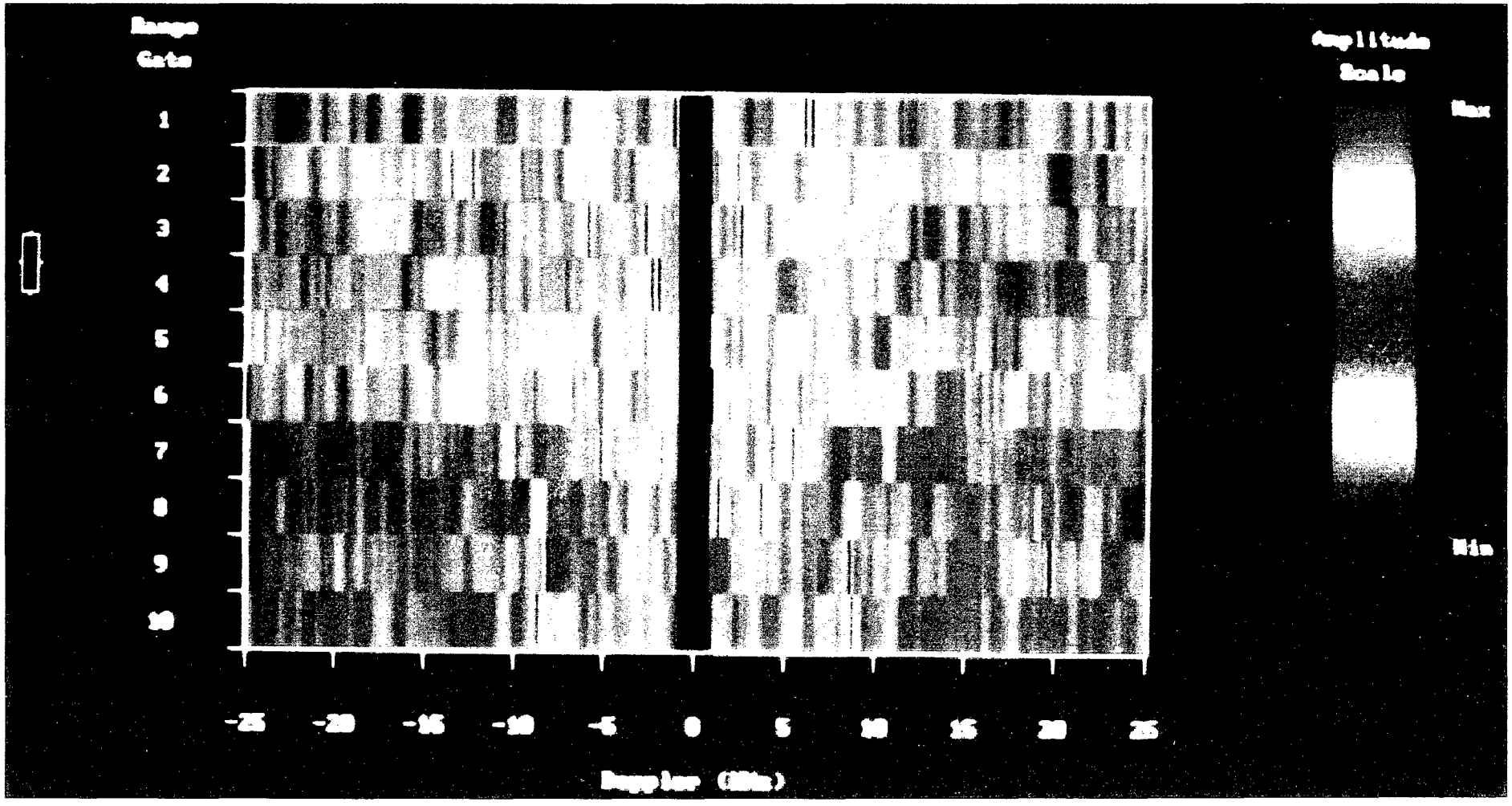

Figure 7.5 - The range cell readout on the Georgia Tech pulsed doppler radar. Note that there is no degradation even for the first cell after the main pulse.